Supplemental Materials

Supplemental Figure 1. Expression analysis of STAT3 enhancing germline variants in purified CD8+ and CD4+CD25+ cells.

(**A**) Purity assessment of isolated $CD8^{+ve}$ T cells and $CD4^{+}CD25^{+ve}$ T_{REGs} from spleens of 8-month old healthy wild-type mice. Pooled cells isolated from several (n= 13) C57bl/6 age-matched mice were evaluated for expression of (**B**) FGFR4 by FACS staining for CD4, CD8, CD25, FOXP3 markers and (**C**) MST1R, CSTN2, AMHR2, SEMA5A, EREG, SPIT2 by immunoblot analyses. Expression analyses of all remaining human germline variants containing a membrane-proximal STAT3 recruiting motif is shown in the Supplementary Table 1.

Supplemental Figure 2. Expression analysis for FGFR4 in T_{REGs} using *Foxp3-GFP* knock-in reporter mice.

Shown are representative images of results from flow cytometry based surface staining for CD4, CD25 and GITR markers and intracellular staining for FGFR4 using directly labeled antibodies. $CD4^{+}CD25^{+}FOXP3^{+}GFP^{+ve}$ T_{REGs} and $CD4^{+}GITR^{+}FOXP3^{+}GFP^{+ve}$ T_{REGs} in blood, mesenteric lymph nodes, spleens and thymus isolated from 7-month old Foxp3-GFP reporter mice were stained for FGFR4 expression using directly PerCP-Cy5.5 labeled rabbit anti-FGFR4 antibody.

Supplemental Figure 3. Expression analysis for phosphorylated STAT3 (Y705) in $CD4^{+}FOXP3^{+ve}$ regulatory T cells in rs351855-A knock-in mice.

(**A**) Triple staining for CD4, FOXP3 and pSTAT3 (Y705) in total splenocytes of $Fgfr4^{G/G}$ (homozygous), $Fgfr4^{G/A}$ (heterozygous) and $Fgfr4^{A/A}$ (homozygous) mice. Expression levels of phosphorylated STAT3 (Y705) was assessed by gating on $CD4^{+}FOXP3^{+ve}$ T_{REGs}.

(**B**) Immunoblot detection of pSTAT3 (Y705), STAT3 and FOXP3 protein levels in purified CD4+CD25-ve and CD4+CD25+ T cells isolated from *Fgfr4*$^{G/G}$ and *Fgfr4*$^{A/A}$ transgenic mice (splenocytes pooled from n=5 mice)

Supplemental Figure 4. Quantification of B cells, monocytes and CD4 T cells in healthy SNP knock-in transgenic mice.

(**A**) Flow cytometry analyses of CD19^{+ve} B cells in bone marrow, thymus, blood, lymph nodes and spleen extracted from *Fgfr4*$^{G/G}$ and *Fgfr4*$^{A/A}$ homozygous mice at 6-8 weeks of age. Date represent percentage of cells (mean ± S.E.M, n = 3-5 mice per group, **p < 0.01, ns = not significant)

(**B**) Flow cytometry analysis of F4/80 positive monocyte/macrophage cells in bone marrow, thymus, blood, lymph nodes and spleen extracted from *Fgfr4*$^{G/G}$ and *Fgfr4*$^{A/A}$ homozygous mice of 6-8 weeks age. Data represent percentage of cells (mean ± S.E.M, n = 3-5 mice per group, ns = not significant)

(**C**) Flow cytometry analysis of CD4^{+ve} T cells in bone marrow, thymus, blood, lymph nodes and spleen extracted from *Fgfr4*$^{G/G}$ and *Fgfr4*$^{A/A}$ homozygous mice at 6-8 weeks of age. Date represent percentage of cells (mean ± S.E.M, n = 3 to 5 mice per group, ns = not significant)

Supplemental Figure 5. Quantification of NK cells and TCRγδ cell in lymphoid organs of healthy SNP knock-in mice.

Flow cytometry based enumeration of CD49b and NKp46 double-positive cells and CD3e and TCRγδ double positive cells in mesenteric lymph nodes, spleen and thymus of 8-month old mice of *Fgfr4*$^{G/G}$ and *Fgfr4*$^{A/A}$ genotypes. First two row panels show representative scatter plot and dot blot images of FACS analyses. Bottom row shows histogram analyses of data obtained from 6 mice per group (mean ± S.E.M, n = 6, ns = not significant, two way ANOVA using Sidak's multiple comparisons test).

Supplemental Figure 6. Quantification of CD8, CD4 and T_{REGs} in healthy SNP knock-in mice.

(**A**) Quantification of $CD8^{+ve}$ and (**B**) $CD4^{+ve}$ T cells by flow cytometry in blood, mesenteric lymph nodes, spleens and thymus isolated from 7-month old mice of the following genotypes: $Fgfr4^{G/G}$, $Fgfr4^{G/A}$ and $Fgfr4^{A/A}$

(**C**) Quantification of regulatory T cells was done by intracellular *staining* for detection of $CD4^{+}GITR^{+}FOXP3^{+ve}$ T cells in blood, mesenteric lymph nodes, spleens and thymus isolated from 7 months mice of following genotypes: $Fgfr4^{G/G}$, $Fgfr4^{G/A}$ and $Fgfr4^{A/A}$.

Data shown in (**C**) were analysed by gating on $CD4^{+}GITR^{+ve}$ T cells (mean ± S.E.M; n = 6, ns = not significant; **p < 0.01, ****p < 0.0001; two way ANOVA using Sidak's multiple comparisons test).

Supplemental Figure 7. Quantitative real time PCR analysis for CD4, CD8 and IL10.

Relative abundance of (**A**) *Foxp3*, (**B**) *Il10*, and (**C**) *Cd8* transcripts in spleens of 6-8 week old $Fgfr4^{A/A}$ and $Fgfr4^{G/G}$ mice, measured by quantitative real time PCR. Data represent relative mRNA expression normalized to *Hprt* expression (mean ± S.E.M, n = 3, **p < 0.01, ****p < 0.0001, ns = not significant).

Supplemental Figure 8. Immunophenotyping analyses of FGFR4 deficient mice.

(**A**) Quantification of CD4+ and CD8+ T cells in the age- and gender-matched 6-8 week old *Fgfr4* wild-type and knock-out mice is shown. Immune phenotyping analysis by quantitative flow cytometry for T cells, B cells, TCRγδ cells, macrophages and NK cell populations in the (**B**) thymus and (**C**) spleen (mean ± S.E.M, n=5, ns= not significant)..

Supplemental Figure 9. In vitro suppression assay under IL10 neutralization.

In vitro suppression assays with CD4+CD25+ T_{REGs} from $Fgfr4^{G/G}$ and $Fgfr4^{A/A}$ mice together with $CD8^{+ve}$ T cells from $Fgfr4^{G/G}$ and $Fgfr4^{A/A}$ mice, respectively. T_{REGs} and CD8 T cells were mixed at different ratios and stimulated using mouse T-activator CD3/CD28

Dynabeads in the presence of mouse recombinant IL10. Three days post stimulation percentages of suppression were determined as described in the Methods section. Data are representative of at three independent experiments. For each experiments cells were isolated from a group of 5 mice of either genotypes and each mixed ratio co-cultivated in replicates of 5 wells (mean ± S.E.M; ns = not significant; *p < 0.05, **p < 0.01, ***p < 0.001, two way ANOVA using Sidak's multiple comparisons test).

Supplemental Figure 10. Immunophenotyping analyses for Th1/Th2/Th17 cells in the tumor bearing transgenic mouse model for non-small cell lung cancer.

Intracellular staining patterns of (**A**) IFNγ, (**B**) IL17A, and (**C**) IL4 in the splenic and tumor infiltrating lymphocytes from 6-month old lung tumor-bearing mice of the following genotypes: *Fgfr4*$^{G/G}$*;SPC-CrafBxB, Fgfr4*$^{G/A}$*;SPC-CrafBxB*, and *Fgfr4*$^{A/A}$*;SPC-CrafBxB*. PMA/Ionomycin stimulated spleen cells and tumor infiltrates were stained for CD4, IFNγ, IL17A and IL4. Representative dot blots from five independent experiments for IL17A and IL4 gated on CD4^{+ve} cell populations is shown. Differential numbers of Th1, Th2 and Th17 cells are shown as percentages (mean ± S.E.M, n = 5, ns = not significant, two way ANOVA using Sidak's multiple comparisons test).

Supplemental Figure 11. Immunophenotyping analyses for Th1/Th2/Th17 cells in tumor bearing transgenic mouse model for breast cancer.

Intracellular staining patterns of (**A**) IFNγ, (**B**) IL4, and (**C**) IL17A in the splenic and tumor infiltrating lymphocytes from breast tumor-bearing mice 5 months post-pregnancy of the following genotypes: *Fgfr4*$^{G/G}$*;WAP-Tgfa, Fgfr4*$^{G/A}$*;WAP-Tgfa*, and *Fgfr4*$^{A/A}$*; WAP-Tgfa*. PMA/Ionomycin stimulated spleen cells and tumor infiltrates were stained for CD4, IFNγ, IL17A and IL4. Representative dot blots from five independent experiments for IL17A and IL4 gated on CD4+ cell populations is shown. Differential numbers of Th1, Th2 and Th17

cells are shown as percentages (mean ± S.E.M, n = 5, ns = not significant, two way ANOVA using Sidak's multiple comparisons test).

Supplemental Figure 12. Graphical summary of this study.

Germline encoded receptor variant such as FGFR4 p.Gly388Arg that enhance the amplitude of STAT3 signaling in regulatory T cells impedes tumor infiltration of $CD8^{+ve}$ T cells by the pleiotropic functions in the immune cells resulting in the general homeostatic suppression of $CD8/T_{REG}$ ratio in vivo.

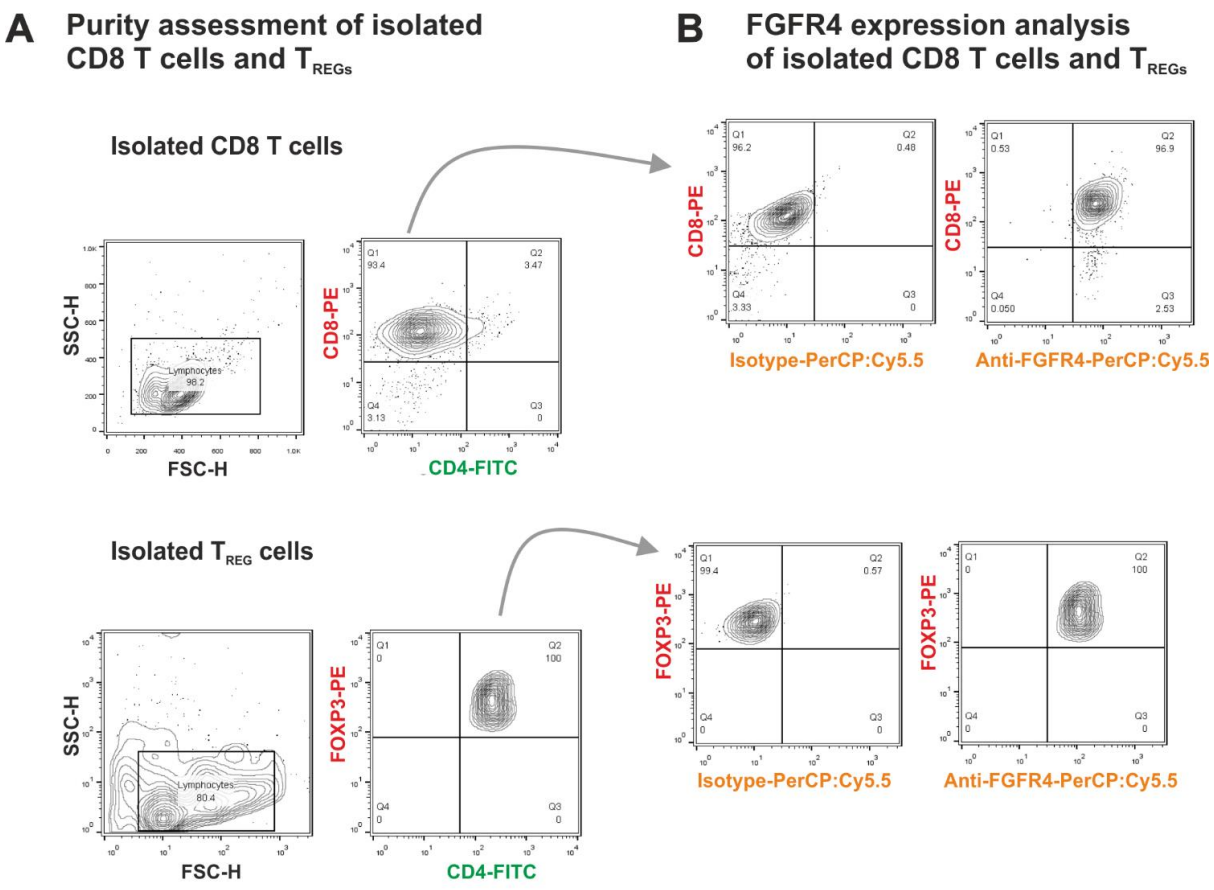

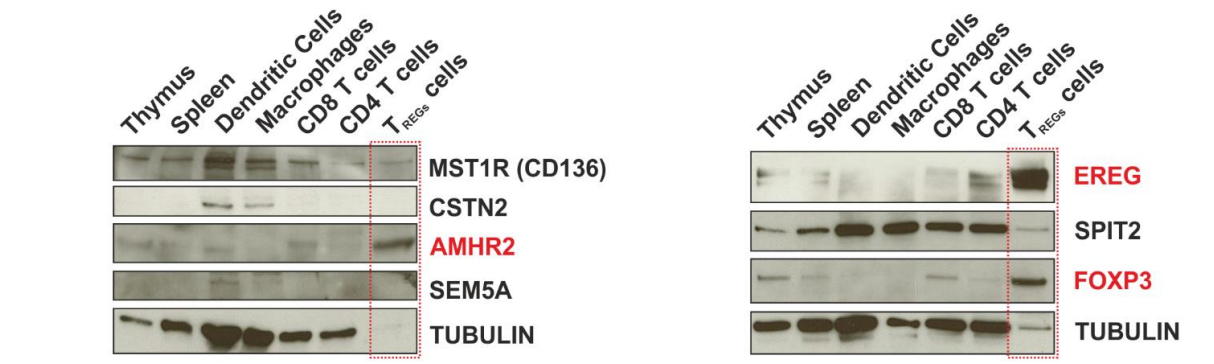

Gene	Uniprot	SNP ID	M.A.F	Ref/Alt Allele	Amino acid Change	Membrane-proximal pTyr Site	'TBSM'	SNP Effect
MST1R (CD136)	Q04912	rs375697146	<0.01	C/T	p.R983Q	980,	'YWWQ'	(CREATED)
CSTN2	Q9H4D0	rs140778211	<0.01	G/A	p.R856Q	853,	'YRVQ'	(CREATED)
AMHR2	Q16671	rs150262652	<0.01	G/A	p.R178Q	175,	'YRVQ'	(CREATED)
SEM5A	Q13591	rs138316526	<0.01	G/A	p.R995Q	992,	'YCQQ'	(CREATED)
EREG	O14944	rs35275884	<0.01	G/A	p.R147Q	144,	'YRNQ'	(CREATED)
SPIT2	O432912	rs148652374	<0.01	G/A	p.R222Q	219,	'YLIQ'	(CREATED)

Please see Supplementary Table. 1 for expression profiling data for remaining STAT3 enhancing germline receptor variants

Supplemental Figure. 1

Expression profiling for FGFR4 (CD334) in regulatory T cells in lymphoid organs of *Foxp3-GFP* knock-in mice

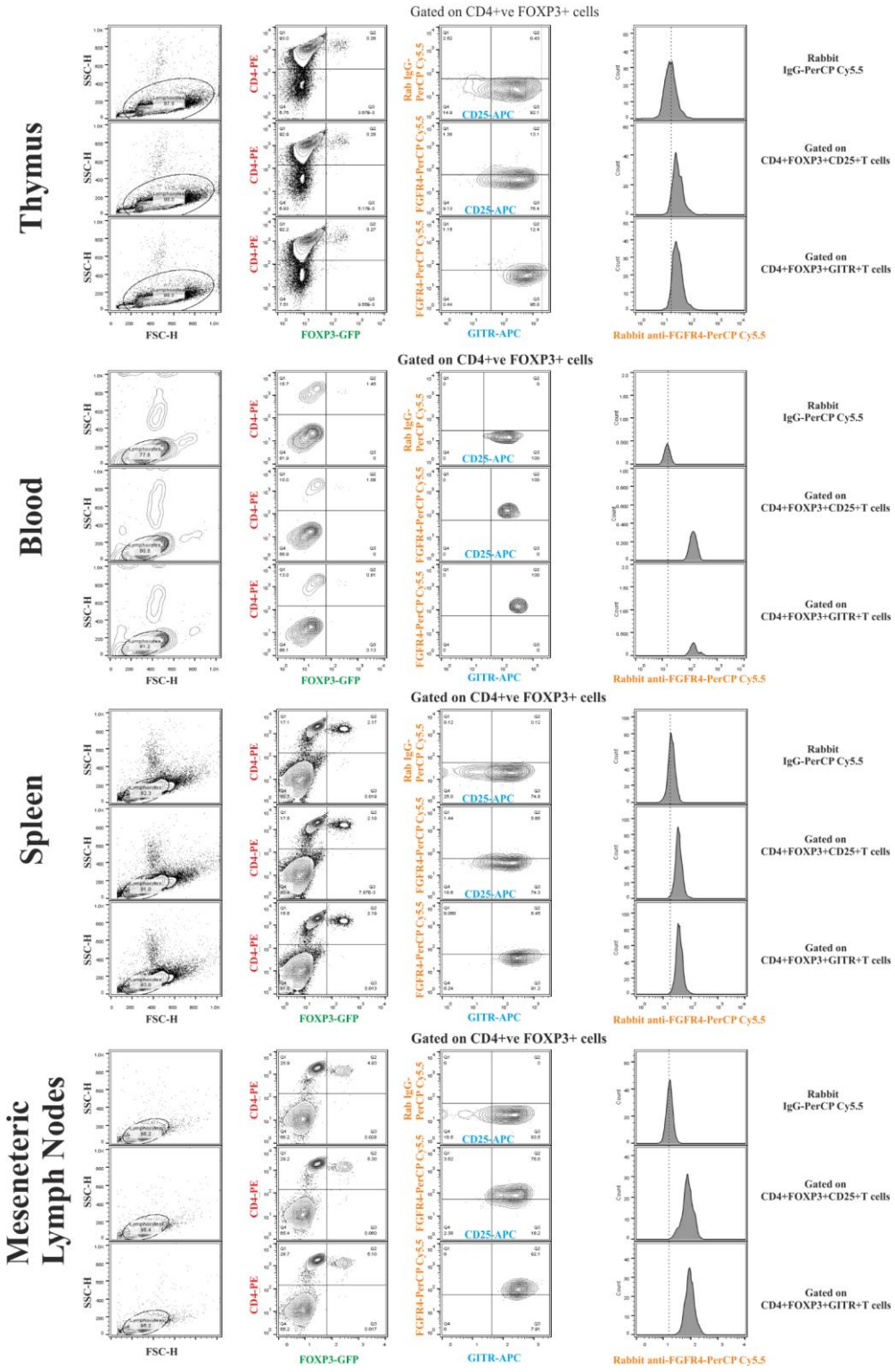

Supplemental Figure. 2

Genotype-dependent levels of pSTAT3 (Y705) in regulatory T cells

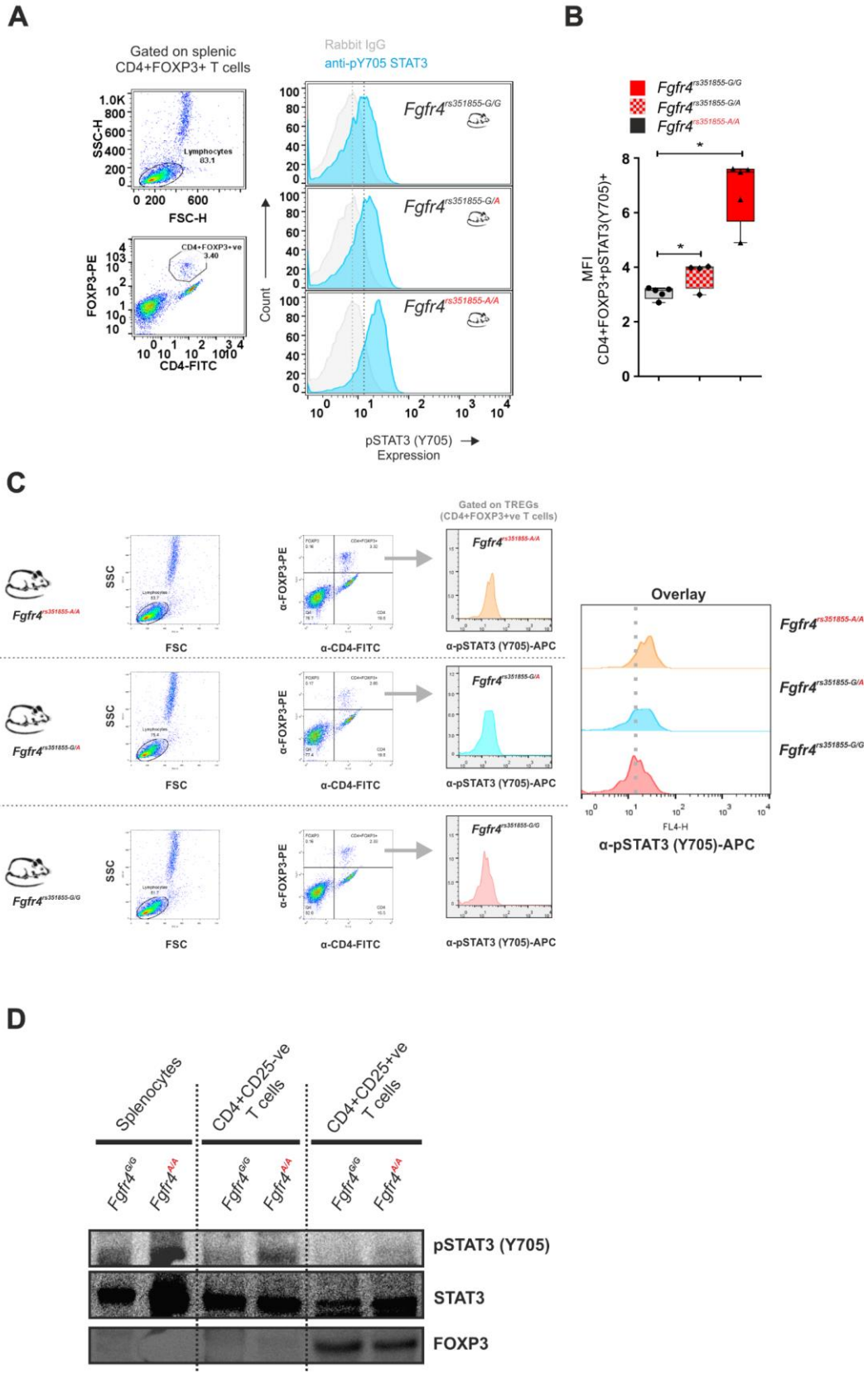

Supplemental Figure. 3

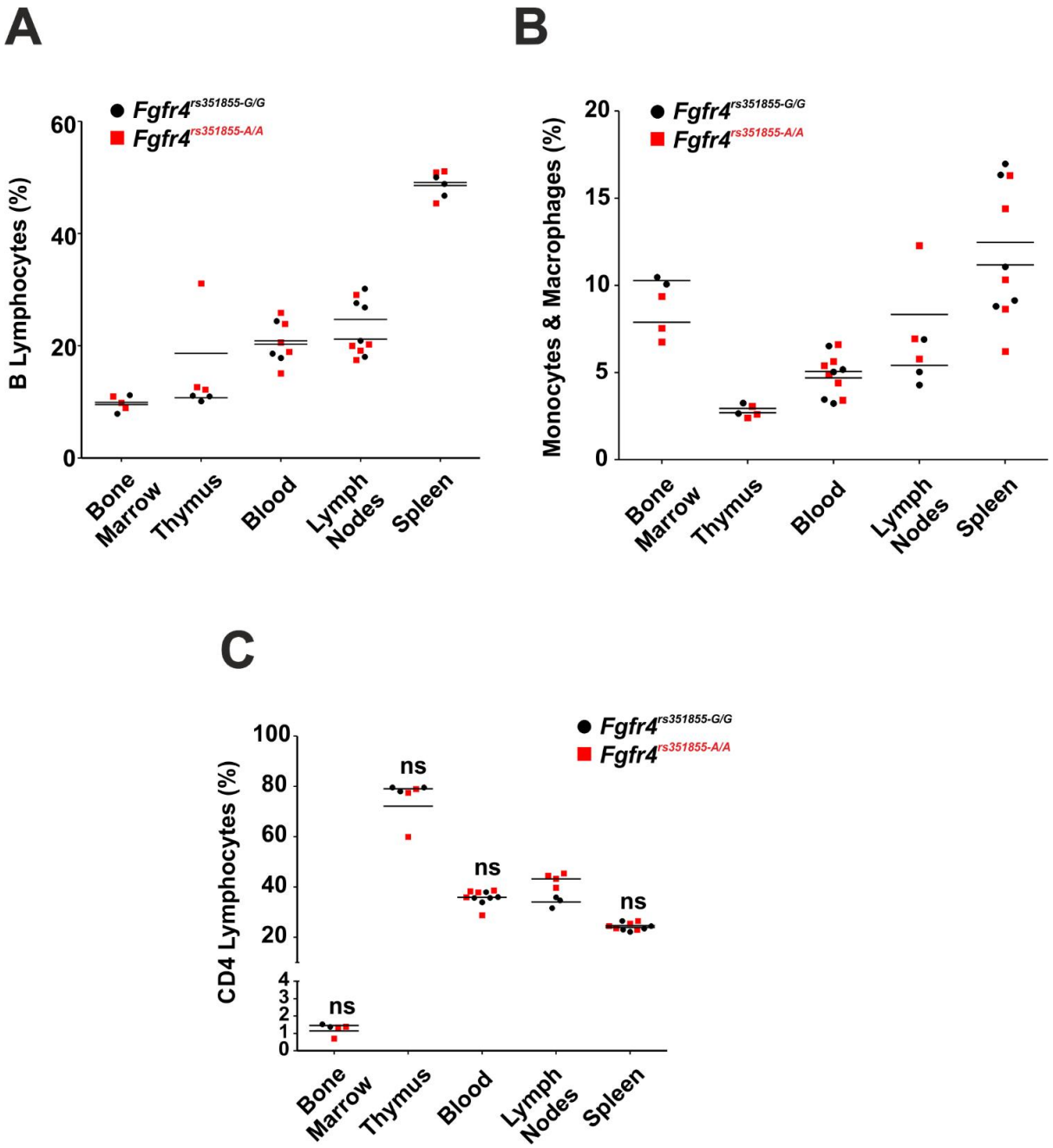

Supplemental Figure. 4

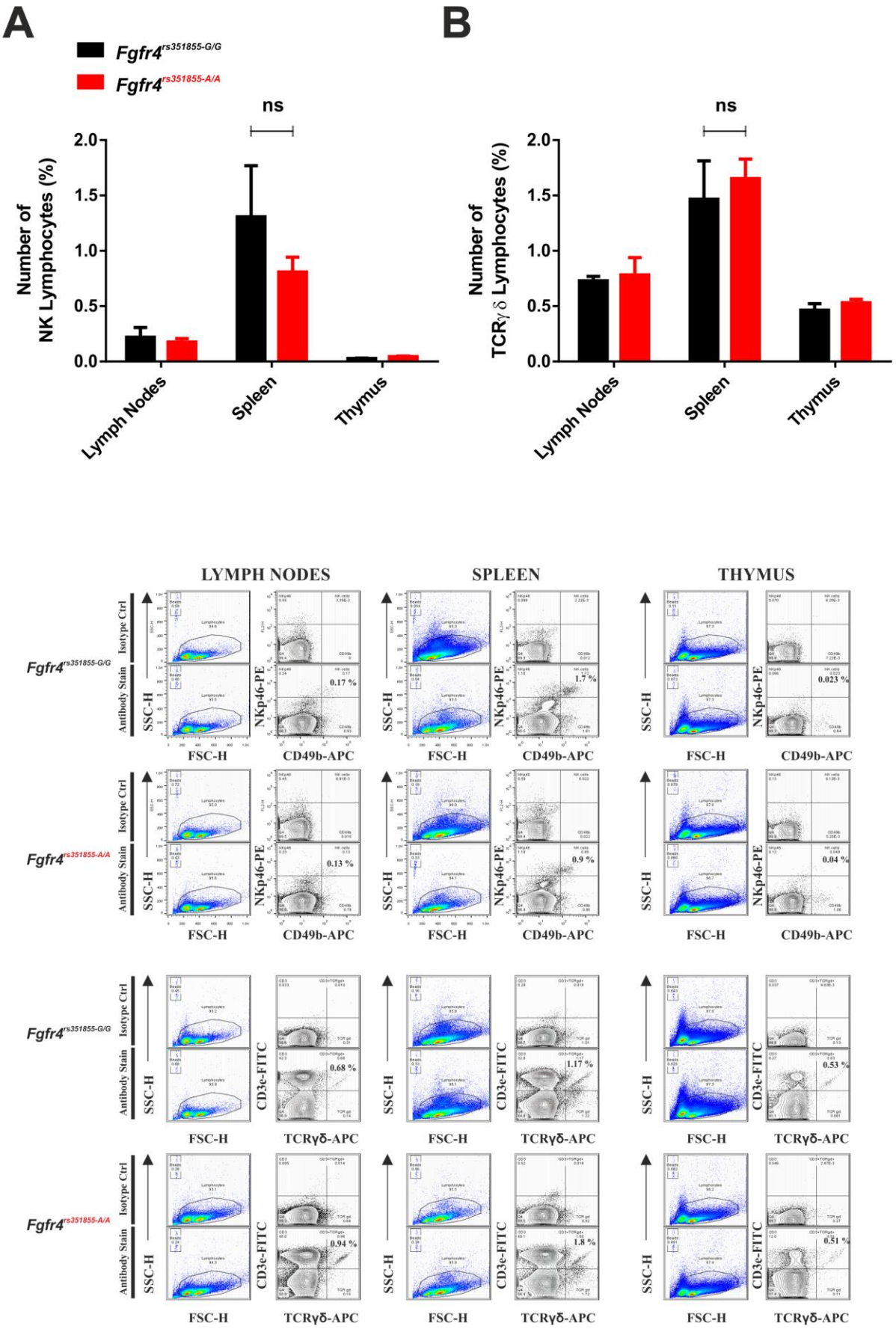

Supplemental Figure. 5

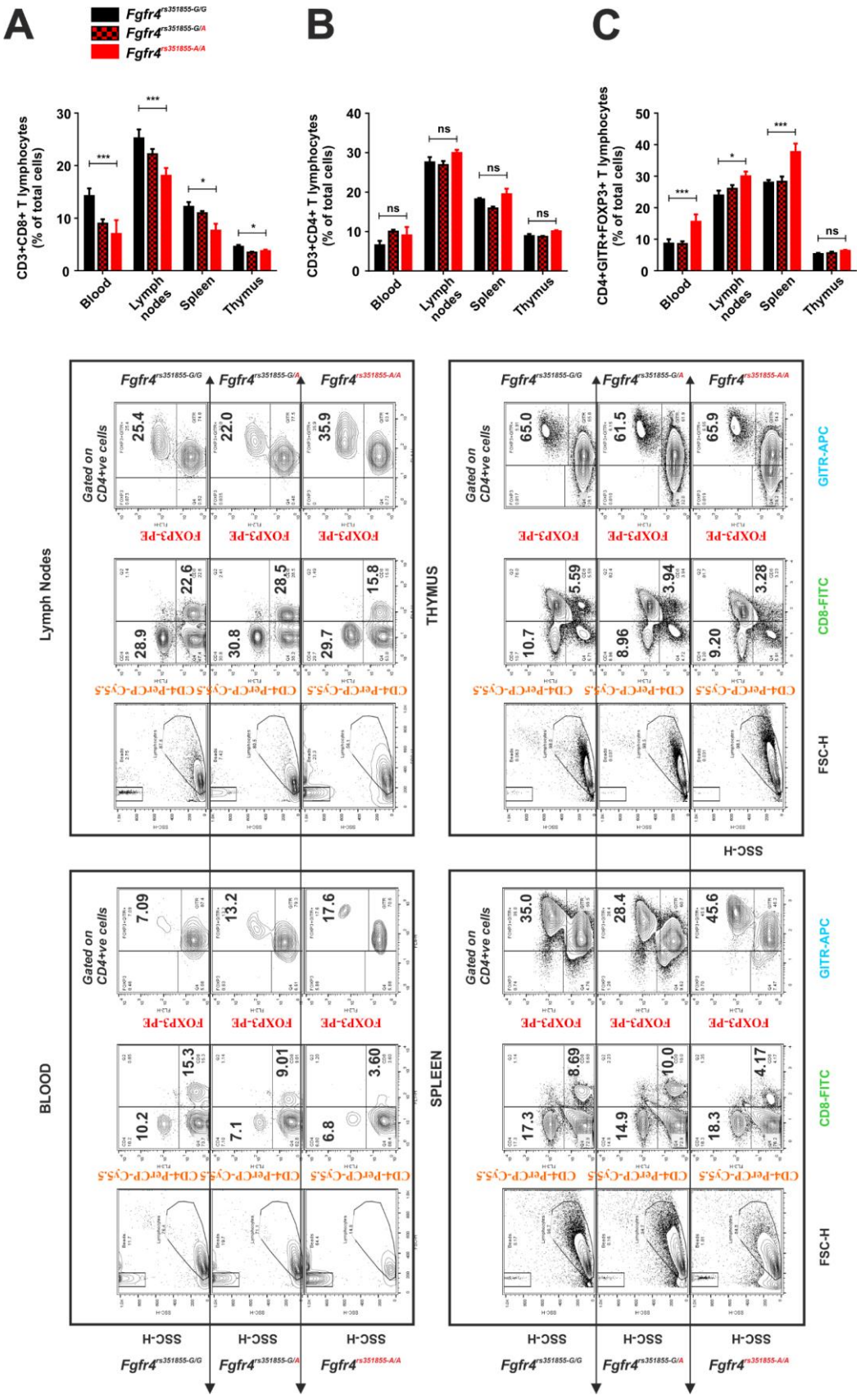

Supplemental Figure. 6

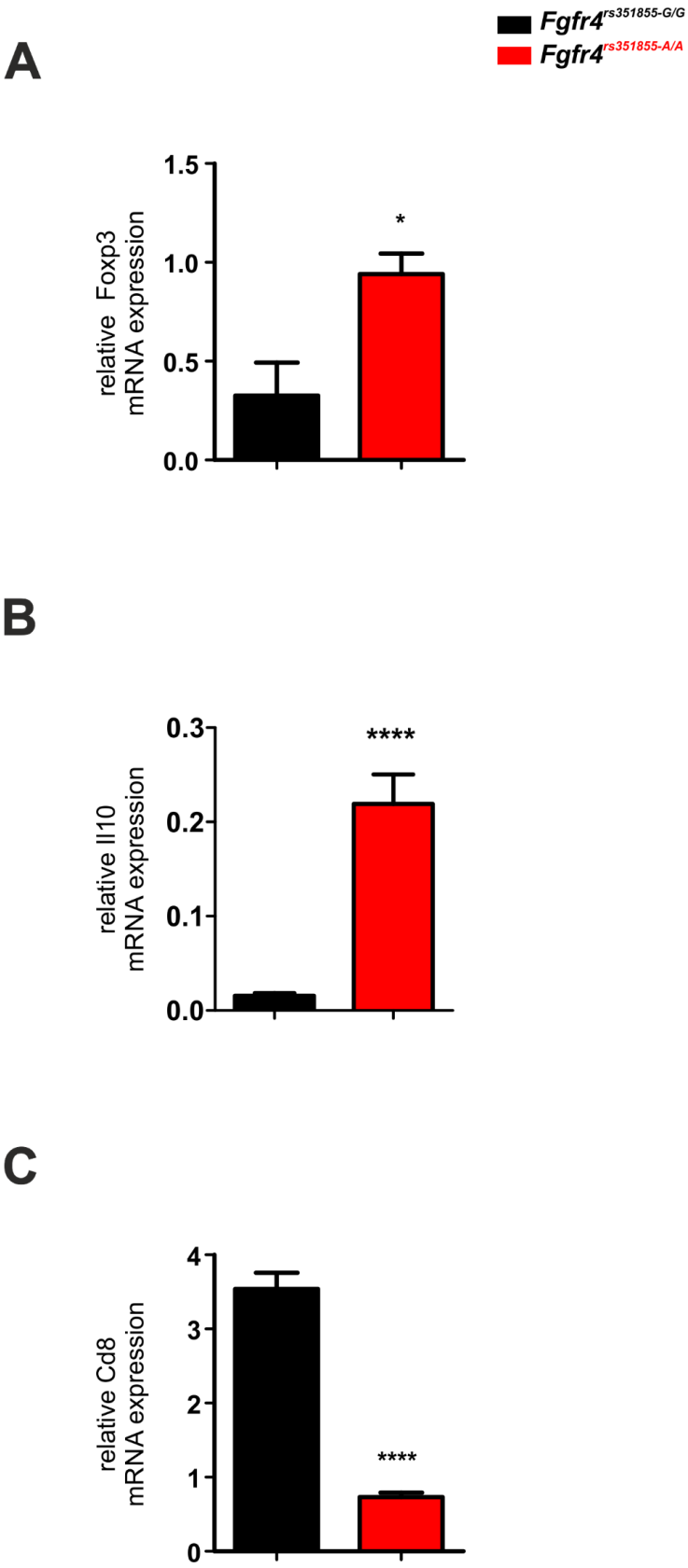

Supplemental Figure. 7

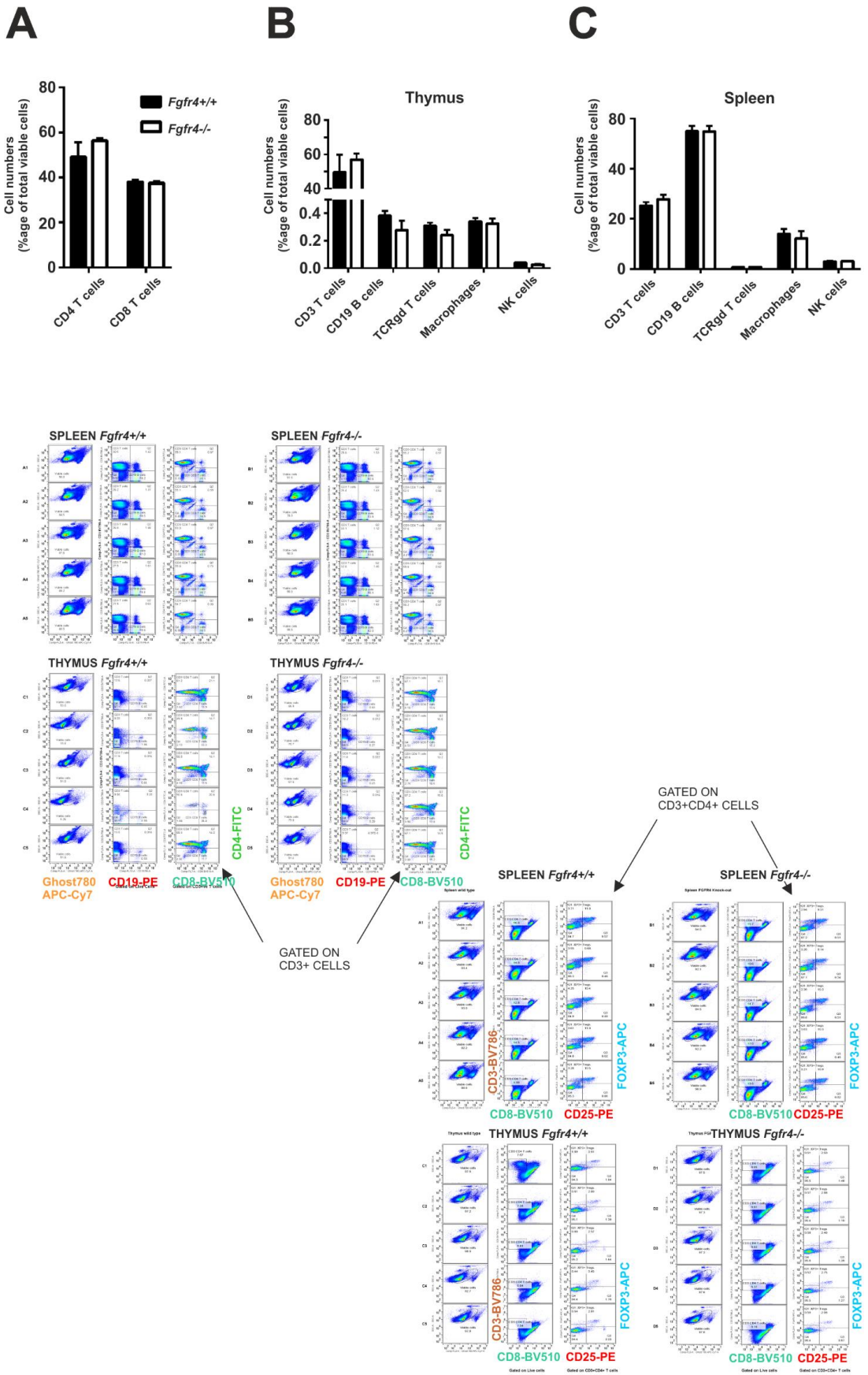

Supplemental Figure. 8

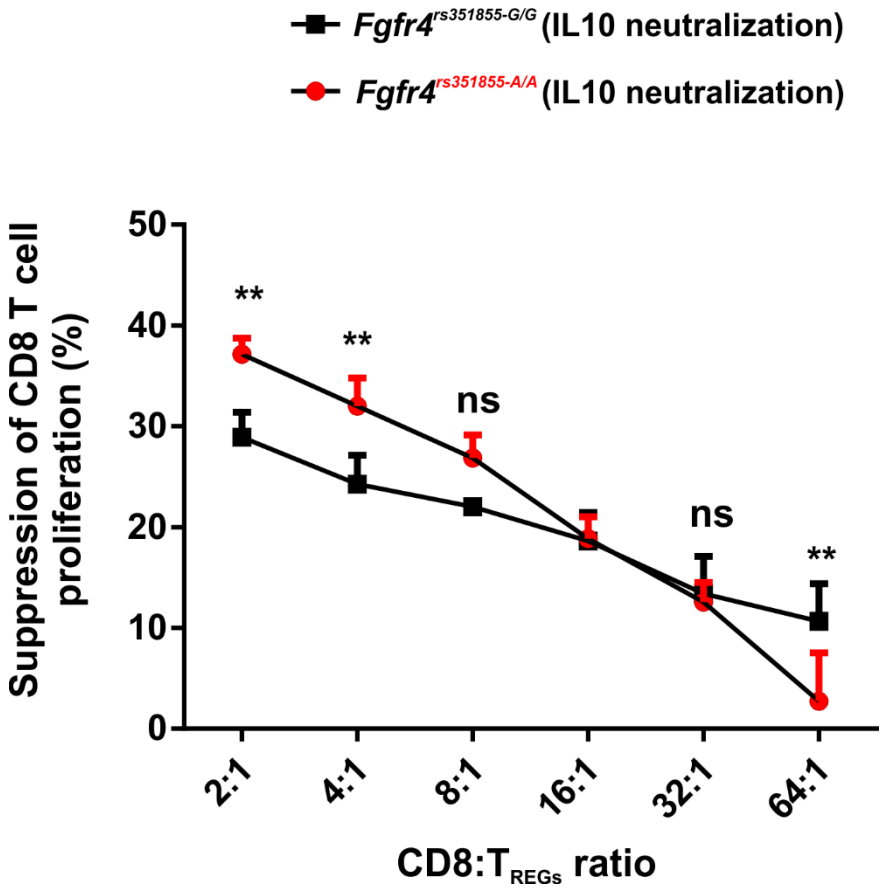

Supplemental Figure. 9

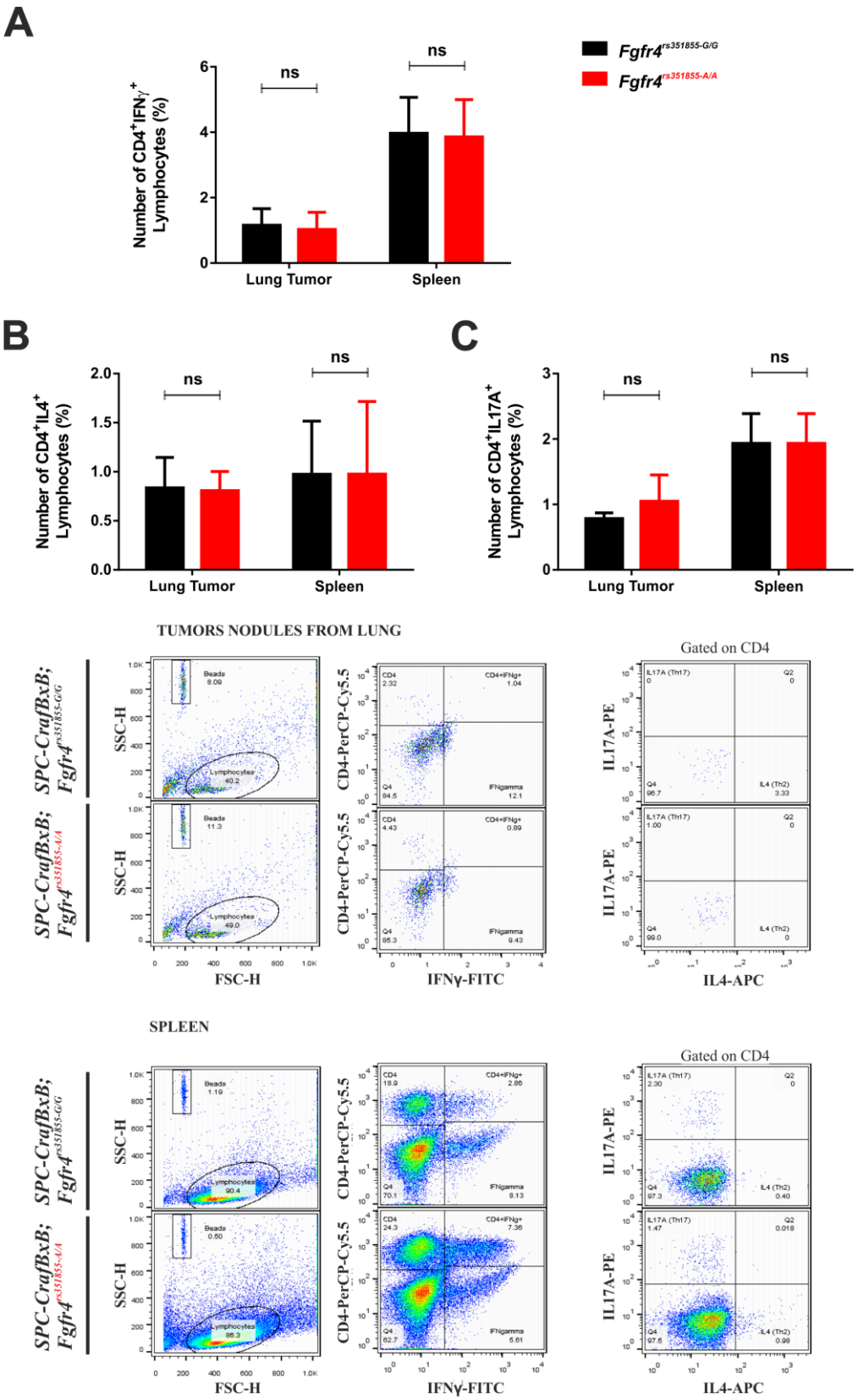

Supplemental Figure. 10

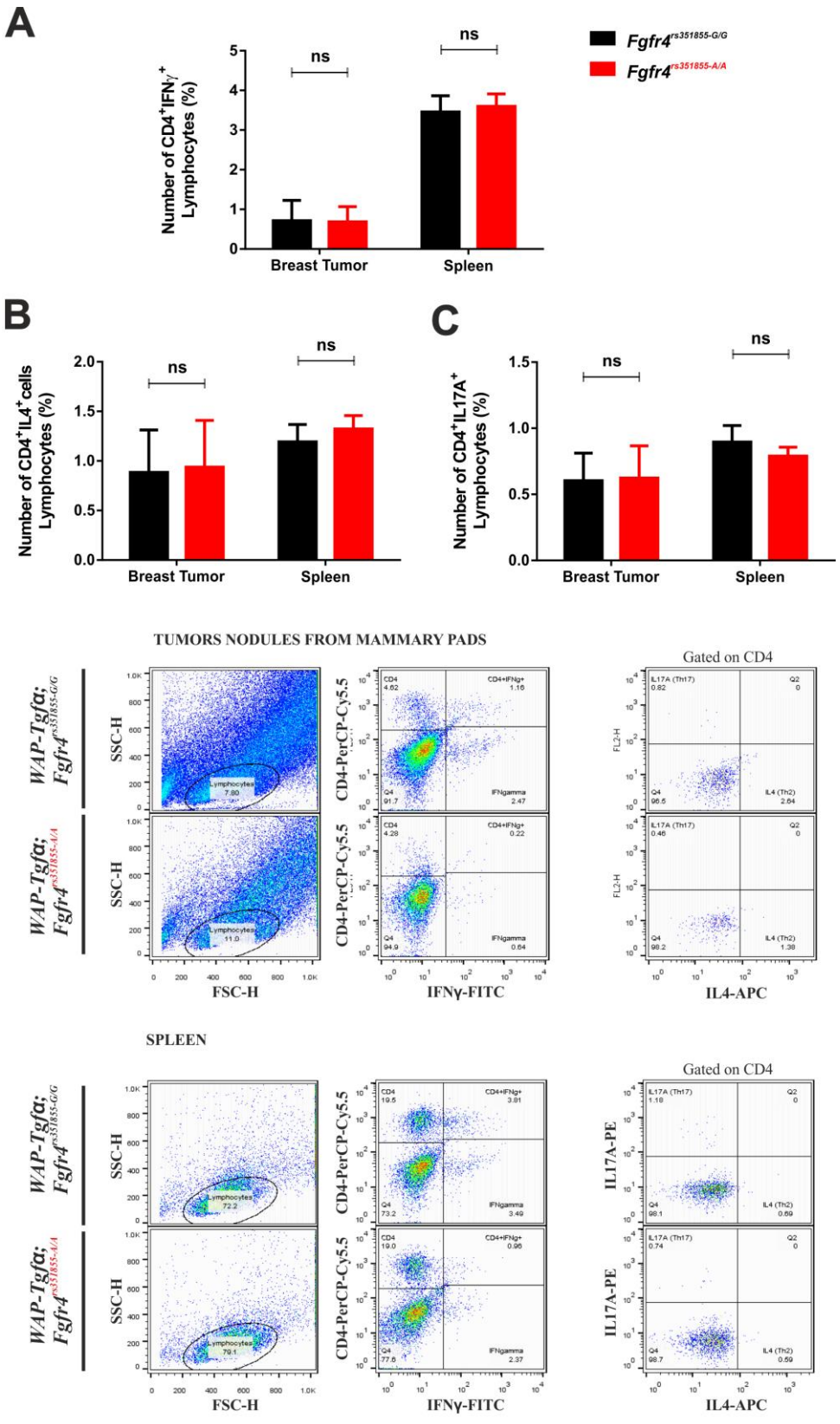

Supplemental Figure. 11

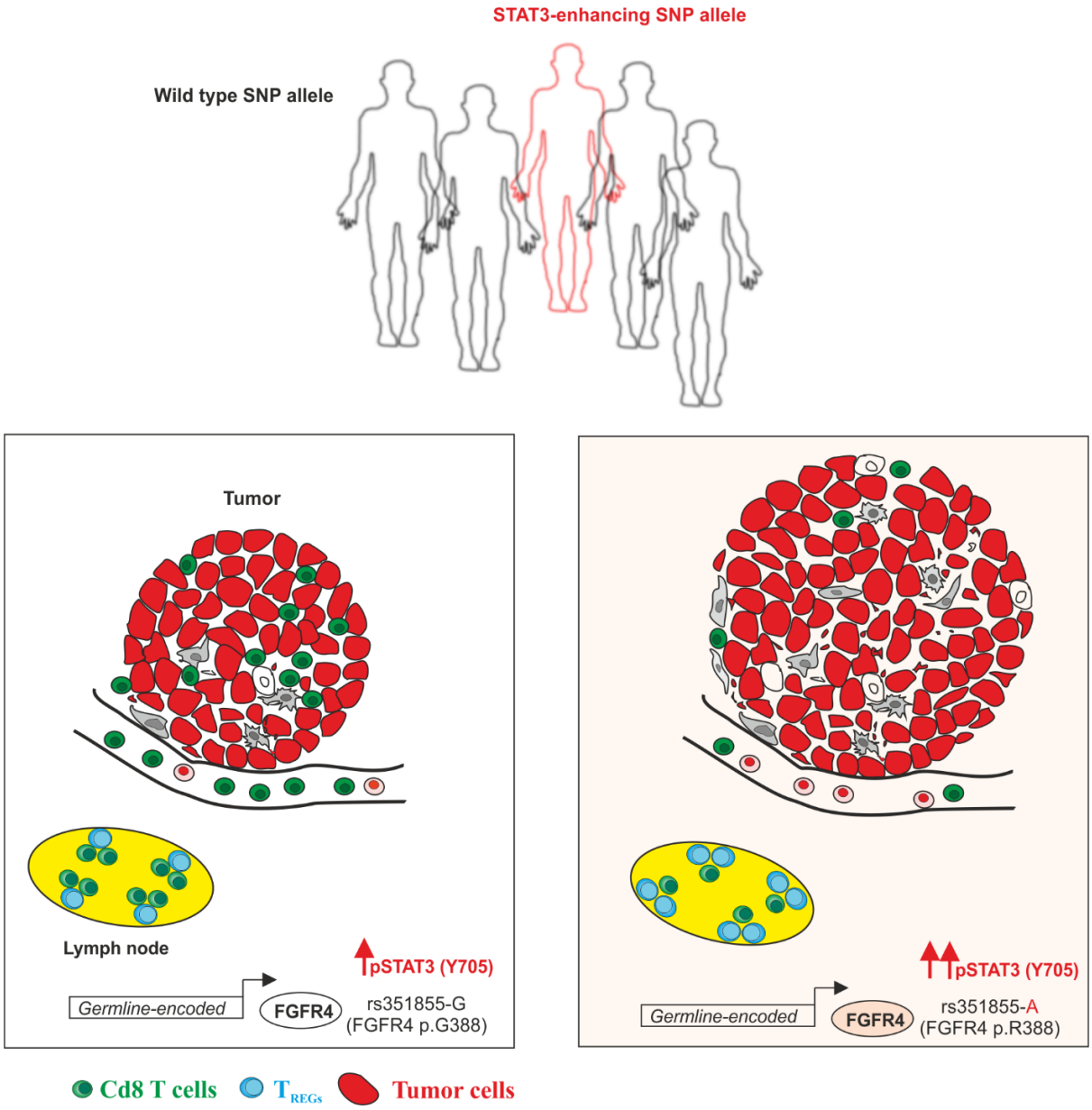

Supplemental Figure. 12

Supplemental Table 1.

Expression analyses by flow cytometry of cell surface receptors in mouse immune cells. Receptors with a germline allele encoding membrane-proximal STAT3 binding sites in humans are listed. MAF = minor allele frequency in the general population. Ref = reference allele and Alt = altered allele.

Kogan et al

S.No	Protein Names	Variation ID	MAF	Ref/ Alt allele	Expression in Immune Subsets	UniProt Accession	Posit-ion	Amino acid change	Mutation type	STAT3 site
1	NRX1B	rs763582196	< 0.01	C/T	CD117+ IL7R- CD150- CD48- AA4.1+ CD43+ HSC BM cells	P58400	393	R->Q	SNP	((390, 'YRNQ'), '[CREATED]')
2	SIGLEC6 (CD327)	rs761002709	< 0.01	G/A	F4/80-hi CD11b-lo CD11c-B220- Macrophages and CD11b+ Gr1+ 7/4hi Neutrophils from BM	O43699	398	H->Y	SNP	((398, 'YQHQ'), '[CREATED]')
3	ABHD6	rs771843813	< 0.01	G/A	CD11c-int CD8a+ CD4+ B220+ Gr+ Plasmacytoid DC	Q9BV23	65	R->Q	SNP	((62, 'YSFQ'), '[CREATED]')
4	SLAF7 (CD319)	rs765616054	NA	A/G	CD11c+ CD8a+ CD4- CD11b- DC	Q9NQ25	261	E->Q	SNP	((258, 'YIEQ'), '[CREATED]')
5	PGFRB (CD140b)	rs140081345	< 0.01	C/T	CD117+ IL7R- CD150- CD48- AA4.1+ CD43+ HSC BM cells	P09619	565	R->Q	SNP	((562, 'YEIQ'), '[CREATED]')
6	VASN	rs766817153	NA	G/A	CD117+ IL7R- CD150- CD48- AA4.1+ CD43+ HSC BM cells	Q6EMK4	600	R->Q	SNP	((597, 'YCVQ'), '[CREATED]')
7	ITB7	rs149623424	< 0.01	C/T	CD4, CD8 and GFP+ (Foxp3 KI mice) CD4+ CD25+ Tregs	P26010	756	R->Q	SNP	((753, 'YDRQ'), '[CREATED]')
8	GYPC (CD236)	rs200062204	< 0.01	A/C	CD115+ MHC+ F4/80-lo, SiglecF-, CD11c+ Macrophages	P04921	88	K->Q	SNP	((85, 'YRHQ'), '[CREATED]')
9	C1QR1 (CD93)	rs752043162	< 0.01	C/T	CD115+ MHCII+ Ly6C+ CD11c+ Macrophages and AA4+ IgM- CD19+ CD43- HAS+ pre-B cells	Q9NPY3	609	R->Q	SNP	((606, 'YRKQ'), '[CREATED]')
10	SIT1	rs761803789	< 0.01	A/T	CD3e+ CD4+ CD8- CD19- CD62L-hi naïve T cells and OT1tg Nave CD8 T cells	Q9Y3P8	93	L->Q	SNP	((90, 'YGNQ'), '[CREATED]')
11	TMIE	rs767118682	< 0.01	G/A	TCR-hi CD4- CD8+ CD24- mature T cells	Q8NEW7	96	R->Q	SNP	((93, 'YLQQ'), '[CREATED]')
12	TACT (CD96)	rs777279191	< 0.01	G/A	CD4, CD8, NK cells, gdT cells	P40200	544	C->Y	SNP	((544, 'YQYQ'), '[CREATED]')
13	FGFR4 (CD334)	rs351855	0.3	G/A	CD45+ MHCII+ CD11c+ CD11b+ DC cells, GFP+ (Foxp3	P22455	388	G→R	SNP	((388, 'YRGQ'), '[EXPOSED]')

Kogan et al

					KI mice) CD4+ CD25+ Tregs					
14	TNFRSF4 (OX40)	rs776902723	< 0.01	C/T	CD19+ B220+ IgM++ AA4- CD23- CD43+ CD5+ B cells	P43489	241	R->Q	SNP	((238, 'YLLQ'), '[CREATED]')
15	SPIT2	rs148652374	< 0.01	G/A	CD45+ MHCII+ CD11c+ CD11b+ DC cells, GFP+ (Foxp3 KI mice) CD4+ CD25+ Tregs	O43291	222	R->Q	SNP	((219, 'YLIQ'), '[CREATED]')
16	STIM1	rs200849173	NA	C/T	GFP+ (Foxp3 KI mice) CD4+ CD25+ Tregs	Q13586	259	H->Y	SNP	((259, 'YDLQ'), '[CREATED]')
17	CADM3	rs771266619	< 0.01	G/A	CD11c+ CD8a- CD4+ CD11b+	Q8N126	357	R->Q	SNP	((354, 'YLIQ'), '[CREATED]')
18	ERBB3 (HER3)	rs765179217	< 0.01	G/A	CD11c-int CD8a+ CD4+ B220+ Gr+ Plasmacytoid DC	P21860	683	R->Q	SNP	((680, 'YLEQ'), '[CREATED]')
19	ITA8	rs561911227	< 0.01	C/A	CD11c+ CD4- CD11b- CD8+ DC	P53708	1051	D->Y	SNP	((1051, 'YREQ'), '[CREATED]')
20	ITB4 (CD104)	rs756905048	< 0.01	G/A	CD45+ MHCII+ CD11c+ CD11b+ DC cells	P16144	765	R->Q	SNP	((762, 'YMLQ'), '[CREATED]')
21	DCBD2	rs115330244	< 0.01	C/T	CD115+ MHC+ F4/80-lo, SiglecF-, CD11c+ Macrophages	Q96PD2	572	R->Q	SNP	((569, 'YWDQ'), '[CREATED]')
22	EPHA4	rs770032654	< 0.01	G/A	CD45+ MHCII+ CD11c+ CD11b+ DC cells	P54764	588	H->Y	SNP	((588, 'YLNQ'), '[CREATED]')
23	LRC25	rs771704758	< 0.01	C/T	CD45+ MHCII+ CD11c+ CD11b+ DC cells, CD115+ B220- Ly6c+ MHCII+ Monocytes, CD115+ MHC+ F4/80-lo, SiglecF-, CD11c+ Macrophages	Q8N386	224	R->Q	SNP	((221, 'YGSQ'), '[CREATED]')
24	MPEG1	rs780878835	< 0.01	C/T	CD45+ MHCII+ CD11c+ CD11b+ DC cells, CD115+ B220- Ly6c+ MHCII+ Monocytes, CD115+ MHC+ F4/80-lo, SiglecF-, CD11c+ Macrophages	Q2M385	680	R->Q	SNP	((677, 'YGTQ'), '[CREATED]'),((708, 'YQEQ'), '[PRESENT]')
25	OSTM1	rs780259047	< 0.01	G/A	CD45+ MHCII+ CD11c+	Q86WC4	306	H->Y	SNP	((306, 'YSEQ'),

					CD11b+ DC cells, CD115+ B220- Ly6c+ MHCII+ Monocytes, CD115+ MHC+ F4/80-lo, SiglecF-, CD11c+ Macrophages					'[CREATED]')
26	SDC3	rs775969974	< 0.01	C/A	CD45+ MHCII+ CD11c+ CD11b+ DC cells, CD115+ B220- Ly6c+ MHCII+ Monocytes, CD115+ MHC+ F4/80-lo, SiglecF-, CD11c+ Macrophages	O75056	422	E->Q	SNP	((419, 'YTLQ'), '[CREATED]')
27	CD68	rs370867284	< 0.01	C/T	CD45+ MHCII+ CD11c+ CD11b+ DC cells, CD115+ B220- Ly6c+ MHCII+ Monocytes, CD115+ MHC+ F4/80-lo, SiglecF-, CD11c+ Macrophages	P34810	349	S->Y	SNP	((349, 'YAYQ'), '[CREATED]')
28	IL6RB (CD130)	rs200816863	< 0.01	G/A	TCR+ CD4- TCRa/b CD122-hi CD44-hi CD25- CD8+ T cells	P40189	662	H->Y	SNP	((662, 'YIAQ'), '[CREATED]')
29	LAMP5	rs781664839	< 0.01	G/T	CD45+ MHCII+ CD11c+ CD11b+ DC cells	Q9UJQ1	272	D->Y	SNP	((272, 'YRSQ'), '[CREATED]')
30	RON (CD136)	rs375697146	< 0.01	C/T	CD115+ MHCII+ F4/80-lo, SiglecF-, CD11c+ Macrophages	Q04912	983	R->Q	SNP	((980, 'YWWQ'), '[CREATED]')
31	SEM6D	rs370361613	< 0.01	G/A	F4/80-hi CD11b-lo CD11c- B220- Macrophages	Q8NFY4	687	R->Q	SNP	((684, 'YCYQ'), '[CREATED]')
32	AXL	rs775803336	< 0.01	G/A	CD45+ MHCII+ CD11c+ CD11b+ DC and F4/80-hi CD11b-lo CD11c- B220- Macrophages	P30530	507	R->Q	SNP	((504, 'YSRQ'), '[CREATED]')
33	FCGR1B (CD64)	rs587642032	< 0.01	C/T	CD115+ B220- Ly6c+ MHCII+ Monocytes	Q92637	245	S->Y	SNP	((245, 'YSLQ'), '[CREATED]')
34	CD302	rs769756355	< 0.01	- / T	F4/80-hi CD11b-lo CD11c- B220- Macrophages	Q8IX05	196	H->Q	frame shift	((193, 'YKKQ'), '[CREATED]')

Kogan et al

35	MEGF9	rs185776336	< 0.01	C/T	Bone Marrow CD11b+ Ly6-G+ Granulocytes	Q9H1U4	544	R->Q	SNP	((541, 'YQNQ'), '[CREATED]')
36	VOPP1	rs760304705	< 0.01	C/A	CD3- NK1.1+ Ly49C/I+ NK cells	Q96AW1	89	P->Q	SNP	((86, 'YPPQ'), '[CREATED]'),((100, 'YTRQ'), '[PRESENT]')
37	TMIGD2 (CD28H)	rs763256697	< 0.01	G/A	CD4, CD8 T cells	Q96BF3	200	R->Q	SNP	((197, 'YRPQ'), '[CREATED]')
38	X3CL1	rs199662906	< 0.01	G/A	CD45+ MHCII+ CD11c+ CD11b+ DC cells	P78423	385	R->Q	SNP	((382, 'YIPQ'), '[CREATED]')
39	SYT15	rs201199533	< 0.01	A/G		Q9BQS2	53	S->Y	SNP	((53, 'YSGQ'), '[CREATED]')
40	ACE (CD143)	rs765069550	< 0.01	C/T		P12821	1293	H->Y	SNP	((1293, 'YGPQ'), '[CREATED]')
41	AMHR2	rs150262652	< 0.01	G/A	CD4+CD25+Tregs	Q16671	178	R->Q	SNP	((175, 'YRVQ'), '[CREATED]')
42	CDHR5	rs538921373	< 0.01	C/T		Q9HBB8	697	R->Q	SNP	((694, 'YGPQ'), '[CREATED]')
43	CN037	rs759882651	< 0.01	T/A		Q86TY3	757	N->Y	SNP	((757, 'YSMQ'), '[CREATED]')
44	CSTN2	rs140778211	< 0.01	G/A		Q9H4D0	856	R->Q	SNP	((853, 'YRVQ'), '[CREATED]')
45	DCC	rs765644105	< 0.01	C/A		P43146	1125	S->Y	SNP	((1125, 'YSAQ'), '[CREATED]')
46	EREG	rs35275884	< 0.01	G/A	CD+CD25+ Tregs	O14944	147	R->Q	SNP	((144, 'YRNQ'), '[CREATED]')
47	ERN2	rs775764629	< 0.01	G/A		Q76MJ5	474	H->Y	SNP	((474, 'YISQ'), '[CREATED]')
48	GLPE	rs17018900	< 0.01	C/T		P15421	78	R->Q	SNP	((75, 'YCIQ'), '[CREATED]')
49	IZUM1	rs778368561	< 0.01	C/A		Q8IYV9	346	D->Y	SNP	((346, 'YSRQ'), '[CREATED]')

Kogan et al

50	K1644	rs146886645	< 0.01	C/T		Q3SXP7	134	R->Q	SNP	((131, 'YLAQ'), '[CREATED]')
51	LRFN3	rs529471562	< 0.01	C/G		Q9BTN0	565	H->Q	SNP	((562, 'YKVQ'), '[CREATED]')
52	LRRT4	rs775079691	NA	G/T		Q86VH4	473	S->Y	SNP	((473, 'YERQ'), '[CREATED]')
53	MMP24	rs149443021	< 0.01	G/A		Q9Y5R2	639	R->Q	SNP	((636, 'YYKQ'), '[CREATED]')
54	NTRK3	rs568926009	NA	C/T		Q16288	459	R->Q	SNP	((456, 'YGRQ'), '[CREATED]')
55	SEM5A	rs138316526	< 0.01	G/A		Q13591	995	R->Q	SNP	((992, 'YCQQ'), '[CREATED]'),((996, 'YQQQ'), '[PRESENT]')
56	SIM14	rs138349269	< 0.01	G/A		Q96QK8	88	H->Y	SNP	((88, 'YNGQ'), '[CREATED]')
57	ZP4	rs768615983	< 0.01	C/T		Q12836	534	C->Y	SNP	((534, 'YPDQ'), '[CREATED]')
58	CADH1 (CD324)	Rs587783048 / rs587782162	NA / < 0.01	C/- and C/T		P12830	731	L->*	frame shift	((741, 'YCPQ'), '[CREATED]')

Methods

Animal models. All mice used for this study were raised in C57BL/6 background. *Fgfr4* knock-in mice previously described (Cancer Res; 70(2); 802–12) used at 8-10 weeks of age. Foxp3-GFP knock in reporter mice was kindly provided by Dr. Kerstin Berer & Dr. Gurumoorthy Krishnamoorthy, Max Planck Institute of Neurobiology, Martinsried, Germany.

A knock-in mouse model for non-small cell lung cancer was generated by breeding $Fgfr4^{A/A}$ and $Fgfr4^{G/G}$ mice with *SPC-CRAF-BxB* mice as described previously (Nature **528**, 570-574). The breeder pairs were kindly provided by Prof. Ulf R. Rapp, Max Planck Institute of Heart and Lung Research, Bad-Nauheim, Germany. *SPC-Craf BxB* induce lung tumors in alveolar type II cells of the lung that can be analyzed from 4 months of age. Five to six months old mice were genotyped and sacrificed for analyses.

A knock-in mouse model for breast cancer was generated by breeding $Fgfr4^{A/A}$ and $Fgfr4^{G/G}$ mice with *WAP-Tgfα* mice as previously described (Nature **528**, 570-574). Only female mice post pregnancy were analyzed. Flow cytometry analyses involving cohorts of wild-type and risk-variant groups of mice were done by sacrificing all the mice on the same day.

All lung cancer and breast cancer mouse models used for tumor analyses were male and females respectively. Tumor-bearing mice were regularly monitored and killed before tumor burden affected their well-being. In the WAP-Tgfα transgenic mouse models for breast cancer, spontaneous tumors that arise in mammary pads are visible and measurable. As per our legal institute permit, the maximum tumor volume permitted in WAP-Tgfα mouse models of breast cancers was 1.500 mm^3 (single tumors); in none of our experiments were these limits exceeded. In the SPC-Craf-BxB

transgenic mouse models for non-small-cell lung cancer, the spontaneous tumor in vivo does not permit measurement in live animals. However, loss of body weight is proportional to tumor burden. The maximum weight loss permitted as per our animal permit was 10% of initial body weight. In none of our experiments with mouse models for lung cancer were these limits exceeded.

Immunophenotyping of *Fgfr4* knock-out mice. Male *Fgfr4* deficient mice and wild type littermates previously described (Cell Metabol; 22(6):1020-32) were sacrificed at 8 weeks of age and immune cells were prepared from thymus and spleen.

Human population genotype data. Human genotype data (germline and somatic) in the variable call formats were gathered and aggregated from publicly available datasets, namely HapMap release 28, Wellderly, dbSNP build 149, 1000 genomes ph3, ExAC.r0.3, NCI-60, TCGA, COSMIC and CCLE. Allele frequencies for germline data were obtained from 1000 genome phase 3 build.

Computational Analyses. Aggregated germline variant datasets and somatic variant datasets (mixing of germline genomic DNA from infiltrated immune cells is always a possibility) were analyzed using Transmembrane Protein Variant Identifier algorithm (TraPS-VarI). Results are available at https://vj-ulaganathan.github.io/TraPS_VarI_SourceData.html. TraPS VarI is a tool to identify membrane-proximal tyrosine-based sequence motifs YxxQ, where Y is tyrosine, Q is glutamine and x any amino acid. The python based module for identifying germline receptor variants of single-pass transmembrane proteins that are capable of modulating in a genotype-dependent manner the STAT3 signaling and drug sensitivity to growth inhibition (https://gitlab.com/VJ-Ulaganathan/TraPS-VarI). The algorithm requires single nucleotide polymorphism genotyping datasets in Variable Call Format 4.0 as input.

Western blot analyses. Whole cell lysates were prepared using 1X Cell Lysis Buffer (Cell Signaling #9803) containing cOmplete, mini, EDTA-free tablets (Roche # 11836170001) and PhosSTOP tablets (Roche #04906837001). Equal protein amounts (20-30 μg) were loaded after a (BCA) assay, were seperated on 4-15% Mini-PROTEAN TGX Gels (Bio-Rad # 456-1083) and subsequently transferred onto nitrocellulose membranes. Blots were blocked in 1X NET-Gelatin buffer (1.5 M NaCl, 0.05 M EDTA, 0.5 M Tris pH 7.5, 0.5 % Triton X-100 and 0.25 g/ml Gelatin) and incubated with primary antibodies overnight at 4º C.

The following antibodies were used for western blotting:

Rabbit anti-FGFR4 (Cell Signaling, #8562; clone-D3B12), rabbit anti-FGFR4 (C-16) (Santa Cruz, #sc-124), mouse anti-FGFR4 (A-10) (Santa Cruz, #sc-136988), rabbit anti-FGFR4 (H-121) (Santa Cruz, #sc9006), rabbit anti-ERK1/2 (Cell Signaling, #4695S; clone-137F5), rabbit anti-pERK1/2 (Cell Signaling, #4376S; clone-20G11), mouse anti-BrdU (Cell Signaling, #5292; clone-Bu20a), rabbit anti-pSTAT3 (Y705) (Cell Signaling, #9145; clone-D3A7), rabbit anti-pSTAT3 (S727) (Cell Signaling, #9134), rabbit anti-STAT3 (Cell Signaling, #4904; clone-79D7), mouse anti-STAT3 (Cell Signaling, #9139; clone-124H6), mouse anti-TUBULIN (Sigma, #9026; clone-DM1A), mouse anti-ADAM22 (BioLegend, #831001; clone-N57/2), rabbit anti-AMHR2 (Life Technologies, #PA5-13900), rabbit anti BMPR1b antibody (Merck-Millipore, #ABD50), rabbit anti-CSTN2 (USB life sciences, #034017), rabbit anti-EPIREGULIN (FL-162) (Santa Cruz, #sc-30215), rabbit anti-NTRK3 (Cell Signaling, #3376; clone-C44H5), rabbit anti-SEM5A (Life Technologies, #PA5-26066), rabbit anti-SPINT2 (Abcam, #ab128926; clone-EPR6283(2)) and FOXP3-HRP antibody (Biorbyt, #orb110190).

Horseradish peroxidase (HRP)-conjugated secondary antibodies, anti rabbit conformation-specific HRP conjugated (Cell Signaling, #5127) and anti-mouse light chain-specific HRP conjugated (Dianova, # 115-035-003) antibodies along with an ECL kit (GE Healthcare/ Amersham Pharmacia Biotech, #32106) were used to detect protein signals. Multiple exposures were taken to select images within the dynamic range of the film (GE Healthcare Amersham Hyperfilm ECL, #28906838). Normalization was done using tubulin bands.

Immunoprecipitation. Transfectants were lysed in 1X Cell lysis buffer (Cell Signaling, #9803) containing containing cOmplete, mini, EDTA-free tablets (Roche # 11836170001) and PhosSTOP tablets (Roche #04906837001). Lysates were cleared and incubated with primary antibody overnight at 4º C. 50 µl of Dynabeads Protein A (#10006d, Life Technologies) was added per sample and incubated at rocking for additional 4 hours. Magnetic bead-bound proteins were separated using a DynaMag-2 magnet (#12321, Life Technologies). After 5 washes, co-immunoprecipitated proteins were extracted in 3X Laemmli Buffer.

Flow cytometry. Single cell suspensions from bone marrow, thymus, lymph nodes, spleen, lungs, blood and tumors were prepared for staining. Erythrolysis by ACK lysis buffer (1.5 M NH_4Cl, 100 mM $KHCO_3$, 10 mM EDTA-Na_2, pH 7.4) was performed for suspensions from blood, spleen and bone marrow. Single cell suspensions of whole lung and breast tissues as well as organ bearing tumors were performed by first slicing the tissue in small pieces and resuspending it in 10 mL of digestion cocktail [0.03 gms of Liberase TM (Roche, #05401119001) and 1.3 mg of DNAse I (Thermo Scientific, #EN0521)] reconstituted in RPMI complete medium. Digestion was performed by gentle agitation at 37º C for 30 minutes.

Single cell suspensions were stained with the following antibodies: Rat IgG2b-FITC/Rat IgG2a-RPE negative control (AbD Serotec, #DC037), rat anti-Mouse CD4-FITC/CD8-RPE (AbD Serotec, #DC034; clone-YTS191.1/KT15), rat anti-CD19-RPE (AbD Serotec, #MCA1439PET; clone- 6D5), rat anti-Mouse F4/80-FITC (BioRad, #MCA497FT; clone-Cl:A3-1), rat anti-mouse CD4-PE (eBioscience, #12-0042-81; clone-RM4-5), rat anti-mouse CD8a-PE (eBioscience, #12-0081-81; clone-53-6.7), rat anti-mouse CD25-PerCP-Cy5.5 (eBioscience, #45-0251-82; clone-PC61.5), rat anti-mouse NKp46-PE (eBioscience, #12-3351; clone-29A1.4), rat IgG2a Isotype Control PE (eBioscience, #12-4321; clone-eBR2a), rat anti-mouse CD49b-APC (eBioscience, #17-5971; clone-DX5), armenian hamster anti-mouse CD3e-FITC (eBioscience, #11-0031; clone-145-2C11), armenian Hamster IgG Isotype Control APC (eBioscience, #17-4888; clone-eBio299Arm), armenian hamster anti-mouse gamma delta TCR-APC (eBioscience, #17-5711-81; clone-eBioGL3 (GL-3, GL3)), rat anti-mouse CD117-APC (eBioscience, #17-1171-82; clone-2B8), rat anti-mouse IL7R-FITC (eBioscience, #11-1271-81; clone-A7R34), rat anti-mouse CD150-PE (eBioscience, #12-1502-82; clone-mShad150), armenian hamster anti-mouse CD48-biotin (eBioscience, #13-0481-81; clone-HM48-1), armenian Hamster IgG Isotype Control, Biotin (eBioscience, #13-4888-81; eBio299Arm), rat anti-mouse CD93 (AA4.1)-biotin (eBioscience, #13-5892-81; clone-AA4.1), rat IgG2b kappa Isotype Control, Biotin (eBioscience, # 13-4031-82; clone-eB149/10H5), rat anti-mouse CD43-biotin (eBioscience, #13-0431-82; clone-eBioR2/60), rat IgM Isotype Control, Biotin (eBioscience, #13-4341-81; clone-eBRM), rat anti-mouse CD11b-APC (eBioscience, #17-0112-81; clone-M1/70), armenian hamster anti-mouse CD11c-PE (eBioscience, #12-0114-81; clone-N418), armenian Hamster IgG Isotype Control, PE (eBioscience, #12-4888-81; clone-eBio299Arm), rat anti-mouse B220-FITC

(eBioscience, #11-0452-63; clone-RA3-6B2), rat anti-mouse Gr1-PerCP (Novus Biologicals, #FAB1037C-100; clone-RB6-8C5), rat anti-mouse CD115-FITC (eBioscience , #14-0112-82; clone-M1/70), rat anti-mouse MHCII-APC (eBioscience , #17-5321-82; clone-M5/114.15.2), rat anti-mouse Ly6C-PE (eBioscience, #12-5932-80; clone-HK1.4), rat anti-mouse IgM-biotin (eBioscience, #13-5790-82; clone-II/41), rat IgG2a kappa Isotype Control, Biotin (eBioscience, #13-4321-82; clone-eBR2a) rat anti-mouse CD24 (HAS)-PerCP-Cy5.5; , #45-0242-82; clone-M1/69), rat anti-mouse CD62L-APC (eBioscience , #17-0621-81; clone-MEL-14), rat anti-mouse CD5-PE (eBioscience , #12-0051-82; clone-53-7.3), rat anti-mouse CD45-PerCP (eBioscience, #MA1-10234; clone-EM-05), rat anti-mouse CD170 (SiglecF) (eBioscience , #14-1702-82; clone-1RNM44N), rat anti-mouse Ly6-G;-biotin (eBioscience , #13-5931-82; clone-RB6-8C5), mouse anti-mouse NK1.1-FITC (eBioscience , #11-5941-81; clone- PK136), mouse IgG2a kappa Isotype Control, FITC (eBioscience, #11-4724-81; clone-eBM2a), syrian hamster anti-mouse Ly49C/1-biotin (eBioscience , #13-5991-81; clone- 14B11), syrian Hamster IgG Isotype Control, Biotin (eBioscience, #13-4914-81), rat anti-mouse CD14-PerCP (eBioscience , #11-0141-81; clone-Sa2-8), armenian hamster anti-mouse CD80-biotin (eBioscience , #13-0801-81; clone-16-10A1) and rat anti-mouse CD86-biotin (eBioscience , #13-0862-81; clone-GL1).

Secondary detection reagents were as follows; Goat anti-Human-APC (Dianova, #109-136-088), donkey anti-Mouse-DyLight488 (Dianova, #715-485-150), goat anti-Rabbit-APC (Dianova, #111-136-144), goat anti-Mouse-APC (Dianova, #115-136-146) and fluorochrome conjugated streptavidin namely PE/Cy7 Streptavidin (BioLegend, #405206), Brilliant Violet 421 Streptavdin (BioLegend, #405226), Brilliant Violet 510 (BioLegend, #504233 and Brilliant Violet 605 (BioLegend, #405229. Rabbit anti-FGFR4 antibody (#136988, Santa Cruz) was directly conjugated

with PerCP Cy5.5 using PerCP Cy5.5 conjugation kit (#LNK142PERCPCY5.5 CJ, AbD Serotec).

Data was analyzed using Flojo Software vX.0.7.

ELISA. IL10 levels in equal volumes of mouse serum samples were quantified using mouse IL10 ELISA ready-set-go kits (eBioscience, #887104-22) by following instructions of the manufacturer.

Immunohistochemistry and immunofluorescence. Tissues were fixed overnight in 4% paraformaldehyde in PBS (pH 7.4) at 4º C. Fixed tissues were embedded in paraffin and sliced. Sections were prepared for staining first by deparaffinization followed by hydration in the following solutions: 3 washes of xylene 5 minutes each, two washes of 100% ethanol 10 minutes each, two washes of 95% ethanol 10 minutes each and two washes in distilled water 5 minutes each. Antigen retrieval was obtained by incubation with heated citrate buffer (sodium citrate 10mM, pH 6) for 15 minutes. Immunohistochemistry was performed as per our standard procedures. Briefly, after antigen retrieval sections were incubated 3% hydrogen peroxide for 10 minutes to quench endogenous peroxidase activity. Non-specific background staining was blocked by incubating in UltraVision Block (Thermo Scientific, # TA-060-PBQ) for 5 minutes at room temperature. Ki67 staining was done by incubating in rabbit anti-Ki67 mAb (Cell Signaling, #9027) at a dilution of 1: 400 overnight at 4º C and CD8 TIL staining was achieved using biotin rat anti-mouse CD88a (BD Pharmingen, #553029, clone-53-6.7 after Fc receptor blocking by mouse 8D Fc block (BD Pharmingen, #553141, clone-2.4G2). For isotype control staining biotin rat IgG2a, κ isotype (BD Pharmingen, #553928) was used. Detection was achieved using HRP Polymer (Thermo Scientific, # TL-060-PH) followed by incubation with peroxidase compatible DAB chromogen.

For immunofluorescence, anti-mouse CD8a-FITC, clone 53-6.7 (eBioscience, # 11-0081-82) was used.

Real Time RT-PCR. Total RNA was isolated using RNeasy Kit (Qiagen, #74104). RNA was reverse transcribed into cDNA by random hexamer with First Strand cDNA Synthesis Kit (Thermo Scientific, #K1622). A StepOne Plus Real Time PCR System (Applied Biosystem) and Fast SYBR Green Master Mix (Life Science Technologies, #4385612) were used for quantitative RT-PCR. Primers used were as follows: mouse

Fgfr4 (forward: 5'-CAAGTGGTTCGTGCAGAGG-3' and

Reverse: 5'-CTTCATCACCTCCATCTCGG-3'),

Cd4 (forward: 5'-CGAACATCTGTGAAGGCAAA-3' and

reverse: 5'- GAGCTCTTGTTGGTTGGGAA-3'),

Cd8 (forward: 5'- GATTGGACTTCGCCTGTGAT-3' and

reverse: 5'- CTTGCCTTCCTGTCTGACTA-3'),

Foxp3 (forward: 5'- GCGAAAGTGGCAGAGAGGTA-3' and

reverse: 5'- GAGGAGCTGCTGAGATGTGA-3'),

Il10 (forward: 5'-TTTGAATTCCCTGGGTGAGA-3' and

reverse: 5'-AGACACCTTGGTCTTGGAGC-3') and

Hprt (forward: 5'- CTTCCTCCTCAGACCGCTTT-3' and

reverse, 5'- TTTTCCAAATCCTCGGCATA-3')

Purification of CD8 and Tregs. CD8+ve T cells, CD4+CD25-Teffector cells and CD4+CD25+ Treg cells were isolated from spleens of mice groups of $Fgfr4^{G/G}$ and $Fgfr4^{A/A}$ genotypes. For each isolation procedures a group consisted of 7 mice. Mice were age and gender matched. For immunoblot analysis of purified CD8+ve T cells, CD4+CD25- Teffector cells and CD4+CD25+ Treg cells, 8-week old wild type C57Bl/6 mice were used for isolation (n = 15 mice). Purified cells were lysed

immediately in 1X Cell Lysis Buffer (#9803, Cell Signaling). All steps taken during isolation procedures were followed as per the manufacturer's guidelines described in Dynabeads® FlowComp™ Mouse CD8 Kit (#11462D, Life Technologies) and Dynabeads® FlowComp™ Mouse CD4+CD25+ Treg Cells Kit (#11463D, Life Technologies).

Generation of bone marrow derived macrophages (BMDM) and dendritic cells (BMDC). The femur bones from both legs of adult mice were carefully rinsed in 70% ethanol before flushing them with cold incomplete medium. The flushes were collected in a centrifugation tube and washed with 50 mL incomplete medium. After ACK erythrolysis cells were washed once in complete RPMI with 10% FCS and 2.5 x 10^6 cells were cultivated in a bacteriological Petri dishes (for non-adhesive surface) in 10 mL complete medium. For BMDM, 1 mL of L929 conditioned medium was added per 10 mL dish on day 0. On day 3, 8 mL of culture medium was replaced with 10 mL fresh conditioned medium (8 mL RPMI with10% FCS and 2 mL L929 medium). On day 6, non-adherent cells were removed and medium was replaced with fresh complete medium. BMDM were harvested on day 8 and lysed for immunoblot analyses. An aliquot was taken for FACS staining using antibodies against CD14, CD11b, CD11c, CD3, CD19, MHCII, CD80 and CD86.

For BMDC, 1 mL of GM-CSF producing hybridoma conditioned medium was added to 10 mL bone marrow culture on day 0. On day 3, medium was replaced with 8 mL RPMI with 10% FCS and 2 mL GM-CSF producing hybridoma conditioned medium. On day 6, old culture medium was once again exchanged with 8 mL RPMI with 10% FCS and 2 mL GM-CSF producing hybridoma conditioned medium. On day 8, BMDC were harvested for immunoblot analyses. An aliquot was taken for FACS

staining using antibodies against CD14, CD11b, CD11c, CD3, CD19, MHCII, CD80 and CD86.

In vitro T_{REG} suppression assay. Treg suppression capacity was evaluated by according to a protocol by Vignali and Colleagues (Methods Mol Biol. (2011; 707: 21–37) with slight modifications. Purified CD8, CD4+CD25+Teff and CD4+CD25+Tregs were assessed for purity followed by staining with proliferation markers, CFSE (#C34554, Life Technologies) for CD8 & Teffs and eFluor670 (#65-0840-85, eBisocience) for Tregs. Counted cells were plated in U-bottomed 96-well plates in desired ratios with same volume of Dynabeads® Mouse T-Activator CD3/CD28 for T-Cell Expansion and Activation (#11456D, Life Technologies) either in presence or absence of mouse IL10 neutralizing antibody, clone JES5-2A5 (#16-7102-81, eBioscience). Relative numbers of CFSE labeled and eFluor670 labeled cells were counted at start and end of experiment viz, day 0 and day 3 respectively using calibrate beads. Percent suppression was calculated using the following formula: ((Numbers of CD8 T cells alone – Numbers of CD8 T cells co-cultivated with T_{REGs})/Numbers of CD8 T cells alone) X 100. To determine statistical significance between groups, two-way ANOVA with a confidence interval of 95% was used.

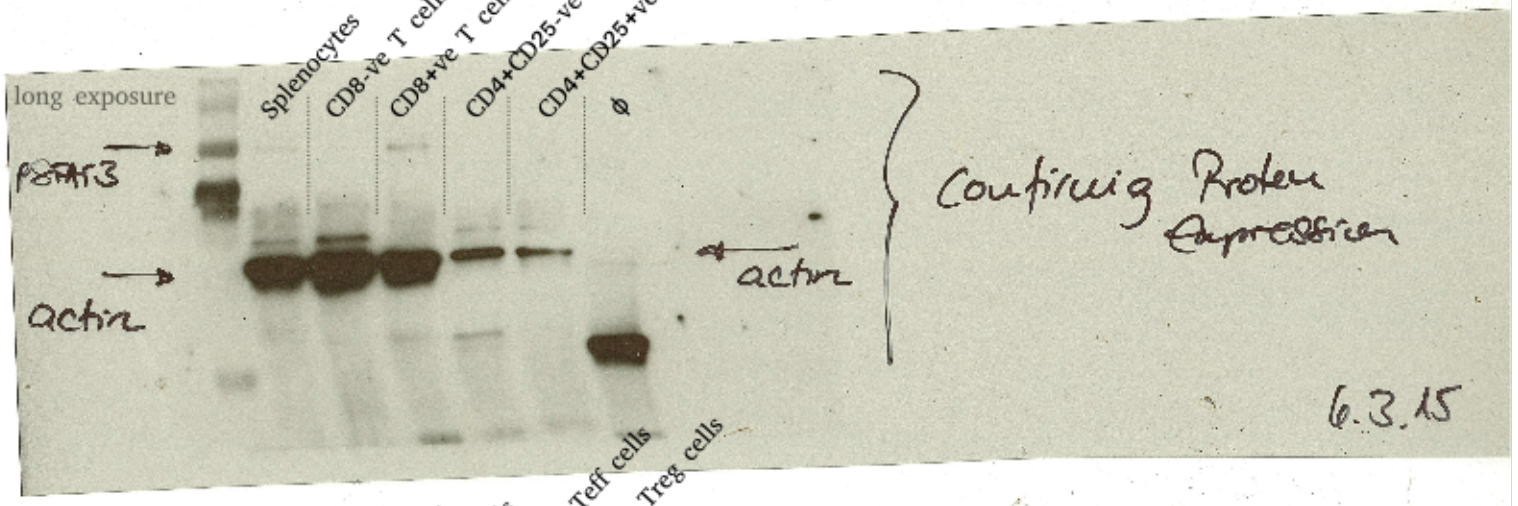

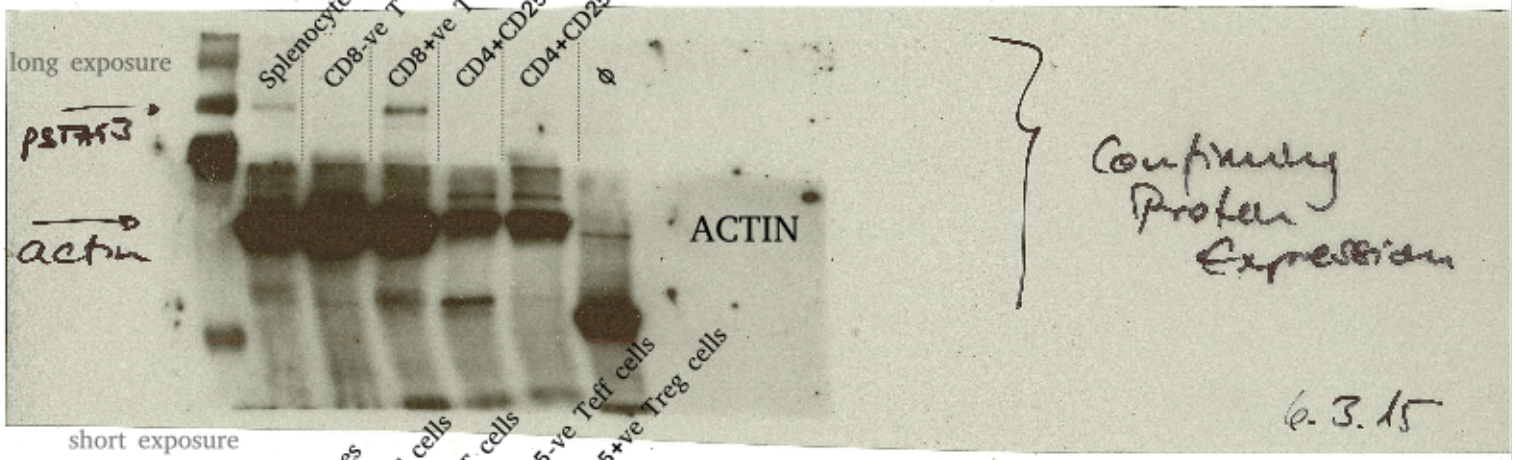

short exposure

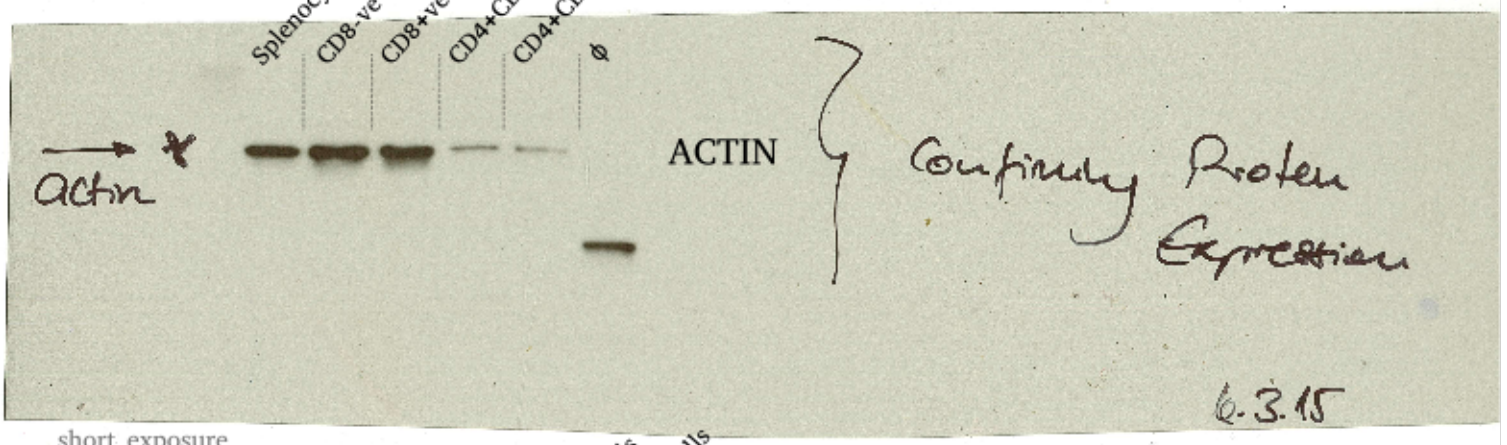

short exposure

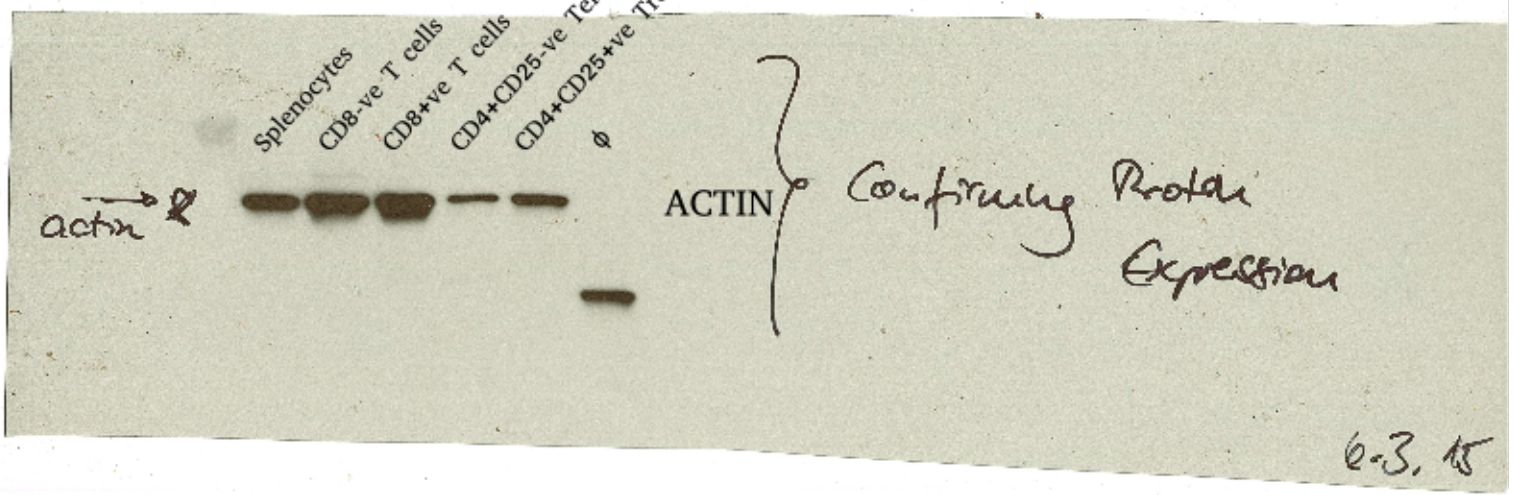

UNCUT GELS PERTAINING TO FIGURE 1A

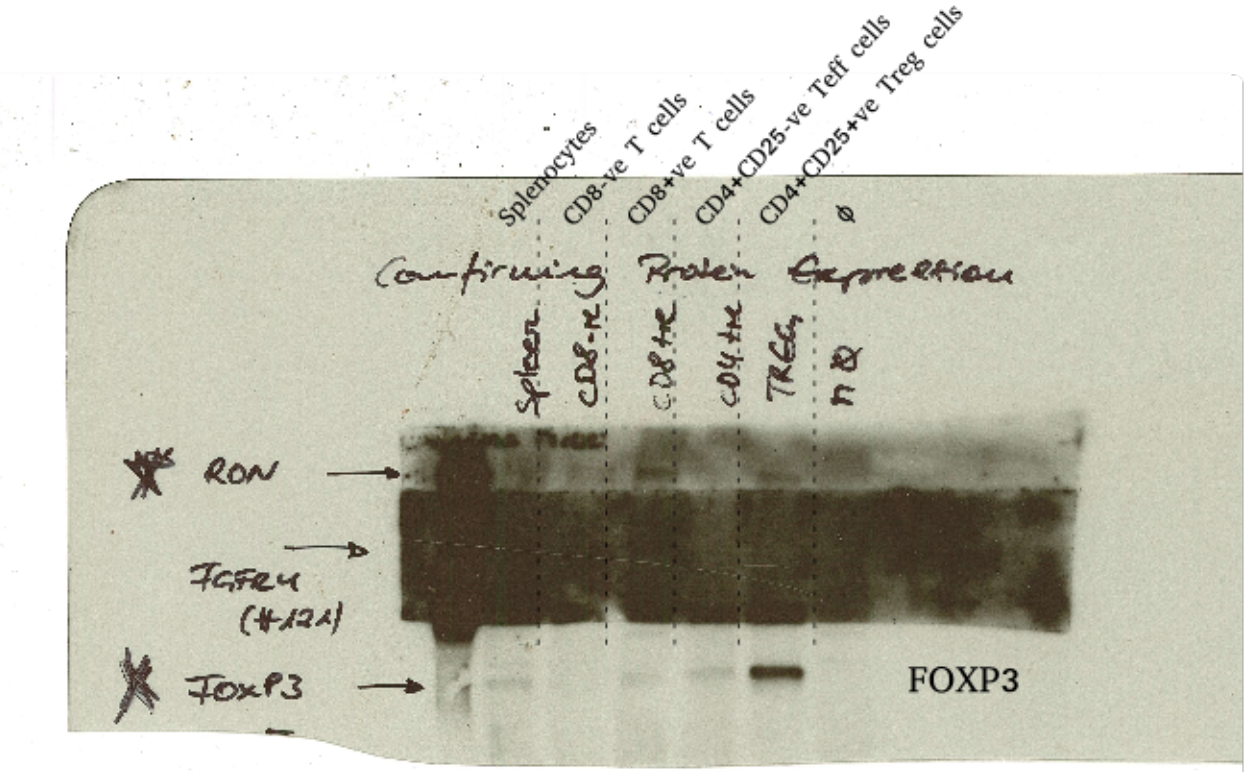

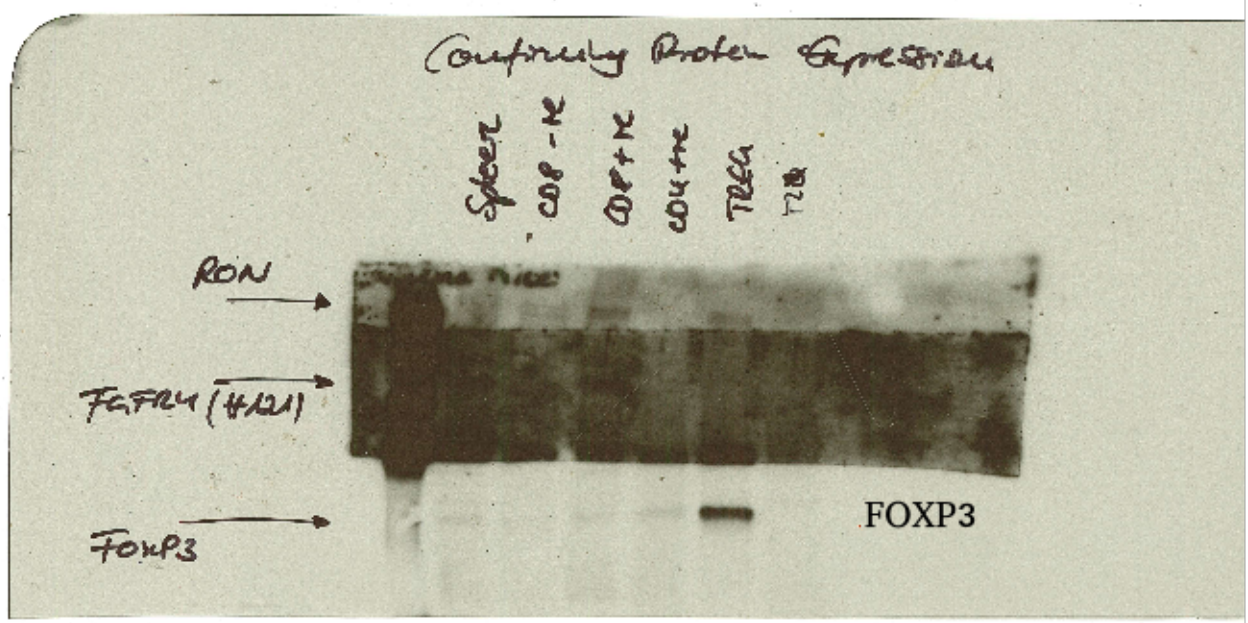

UNCUT GELS PERTAINING TO FIGURE 1A

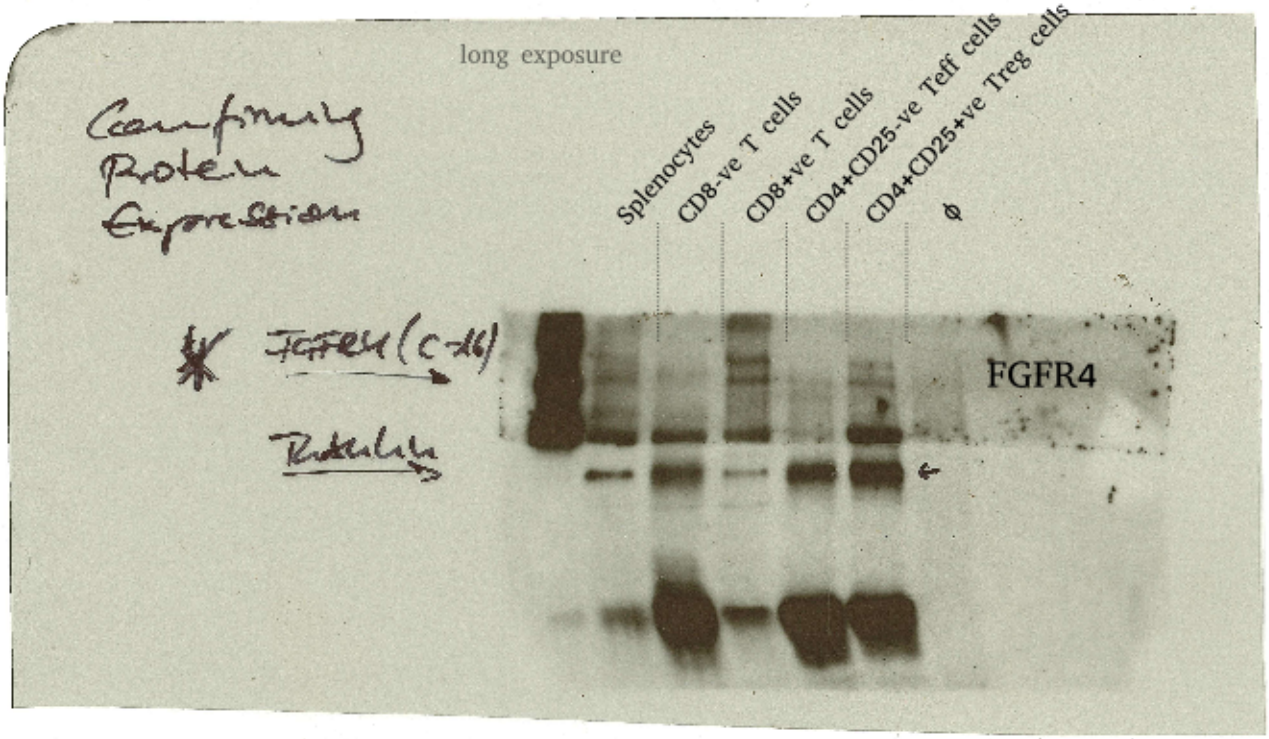

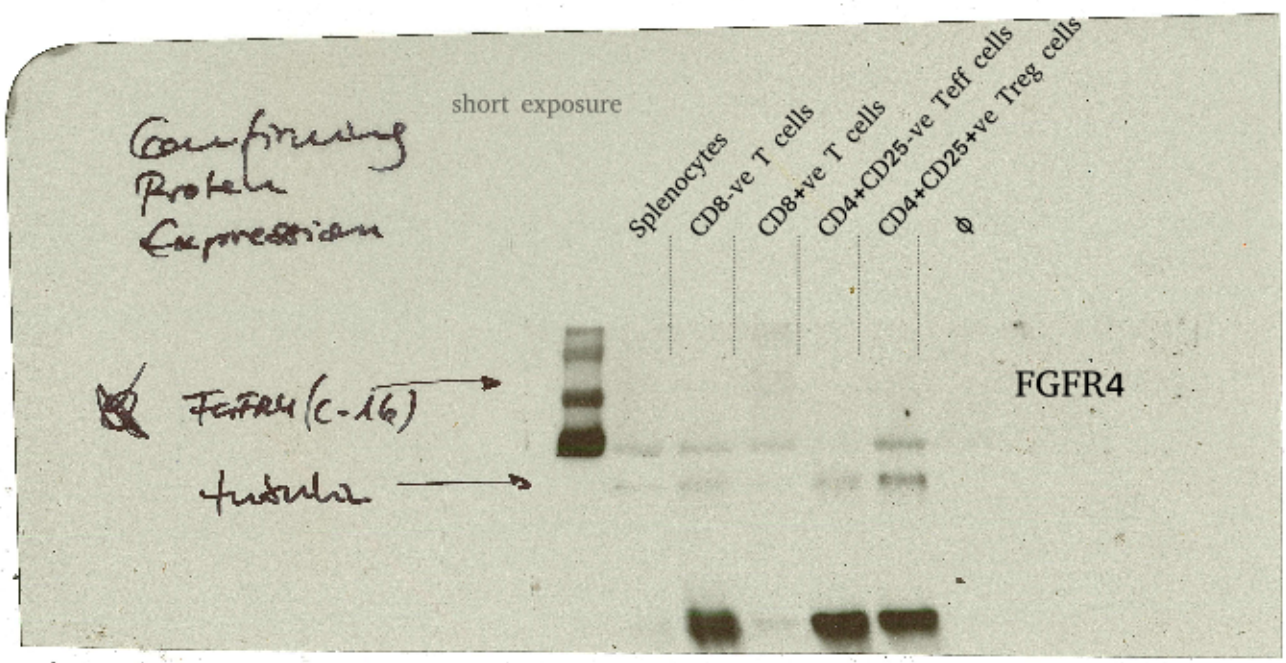

UNCUT GELS PERTAINING TO SUPPLEMENTAL FIGURE 1C

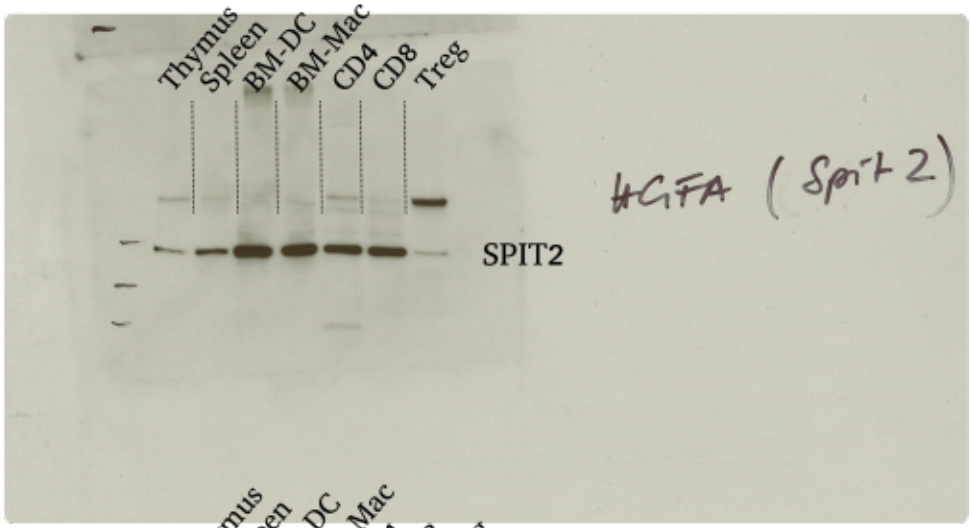

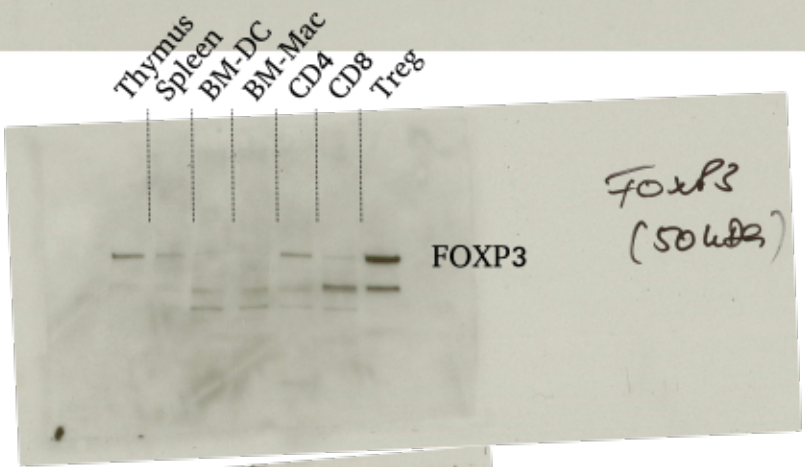

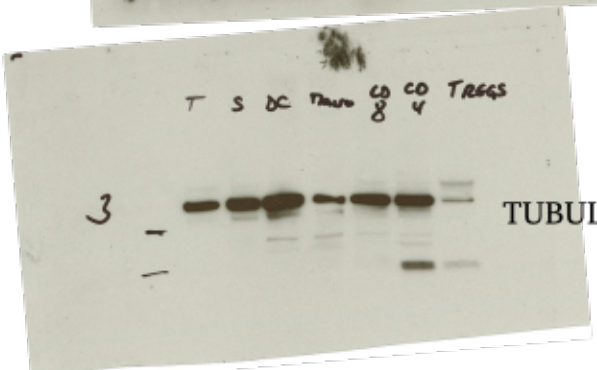

UNCUT GELS PERTAINING TO SUPPLEMENTAL FIGURE 1C

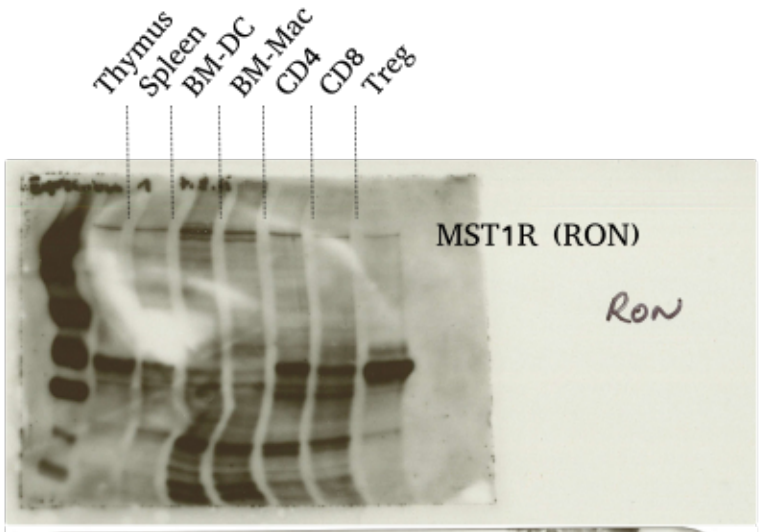

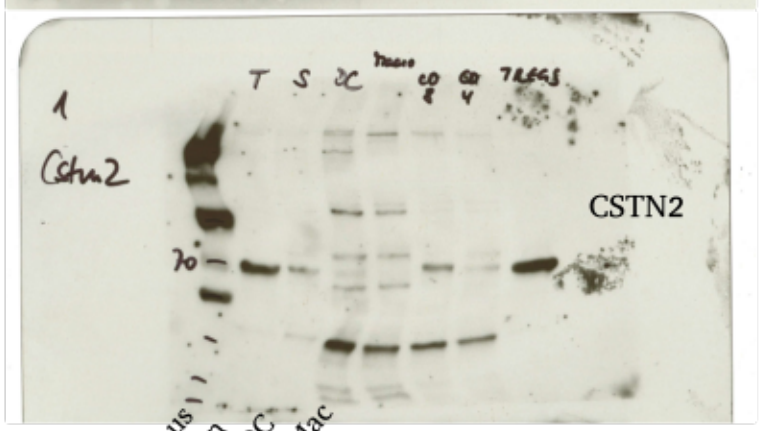

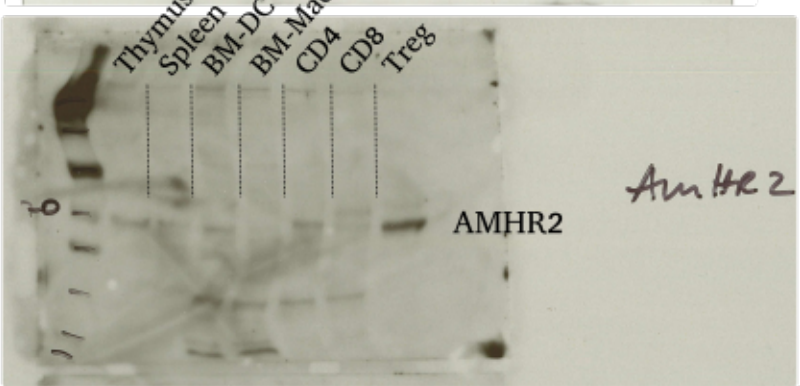

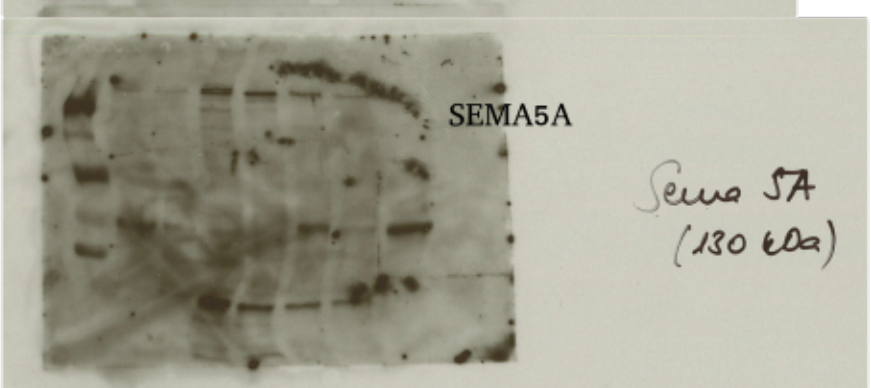

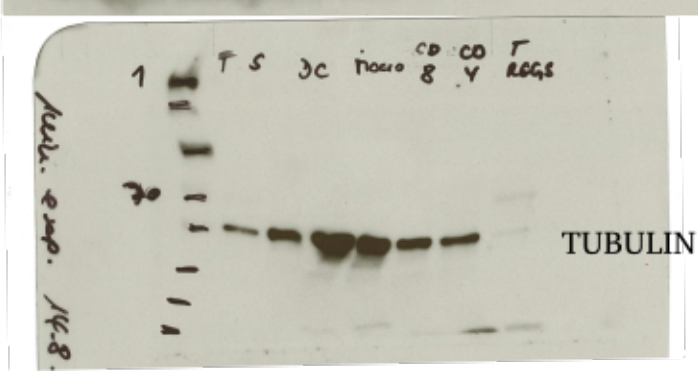

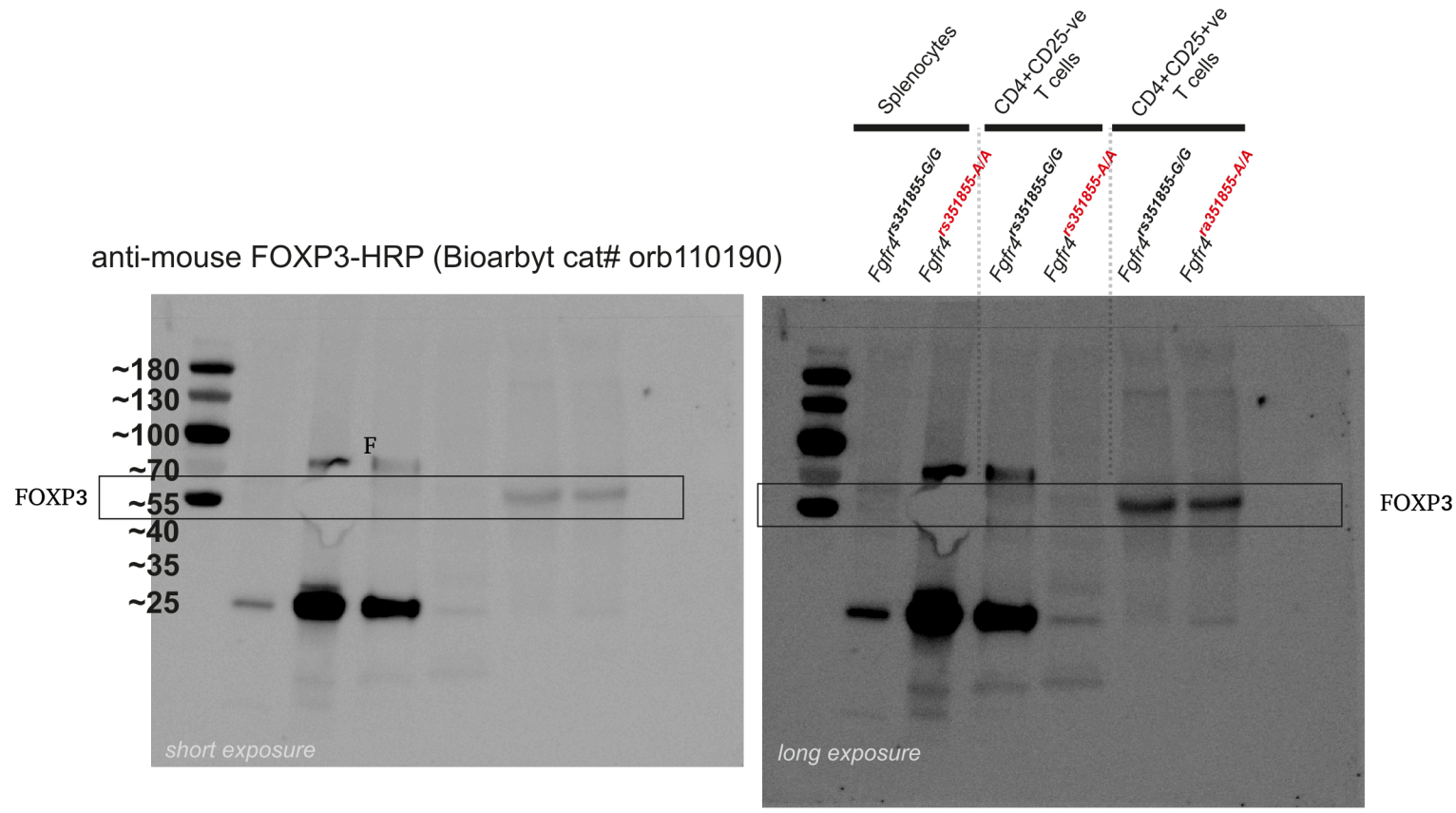
Splenocytes
CD4+CD25-ve T cells
CD4+CD25+ve T cells
Fgfr4rs351855-G/G
Fgfr4rs351855-A/A
Fgfr4rs351855-G/G
Fgfr4rs351855-A/A
Fgfr4rs351855-G/G
Fgfr4ra351855-A/A
anti-mouse FOXP3-HRP (Bioarbyt cat# orb110190)
~180
~130
~100
~70
~55
~40
~35
~25
F
FOXP3
short exposure
long exposure
FOXP3

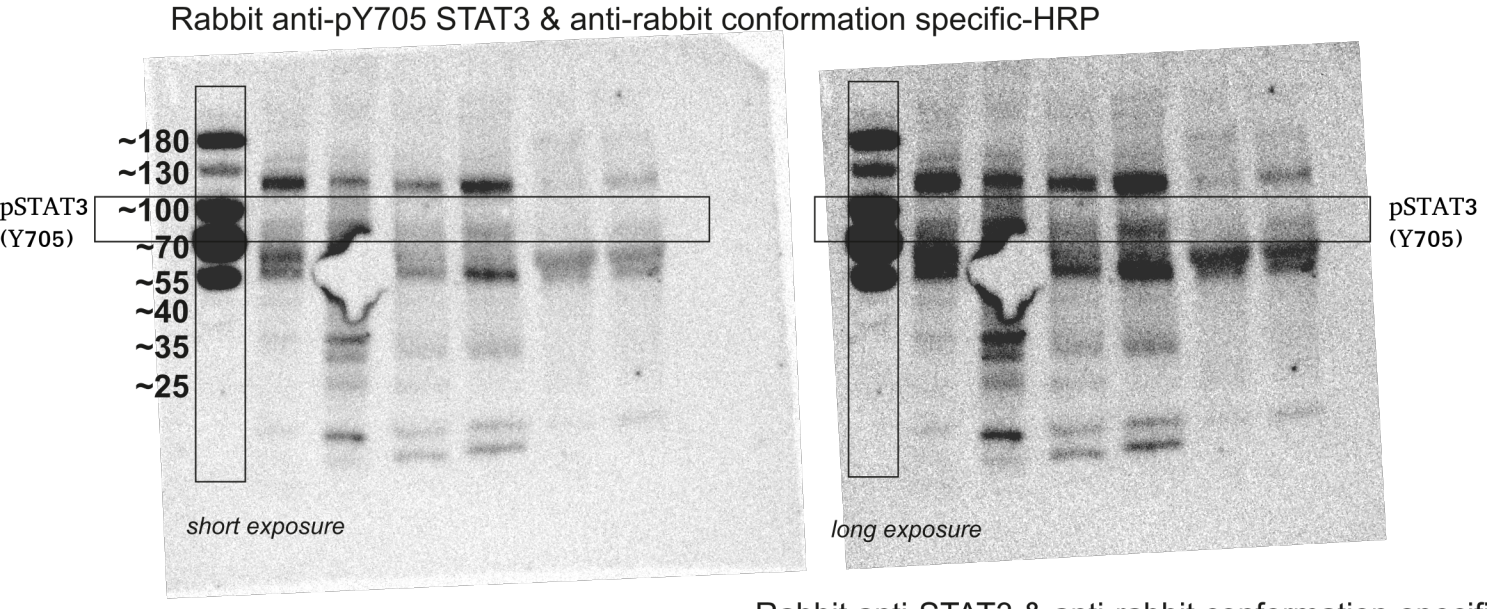
Rabbit anti-pY705 STAT3 & anti-rabbit conformation specific-HRP
~180
~130
~100
~70
~55
~40
~35
~25
pSTAT3 (Y705)
short exposure
long exposure
pSTAT3 (Y705)

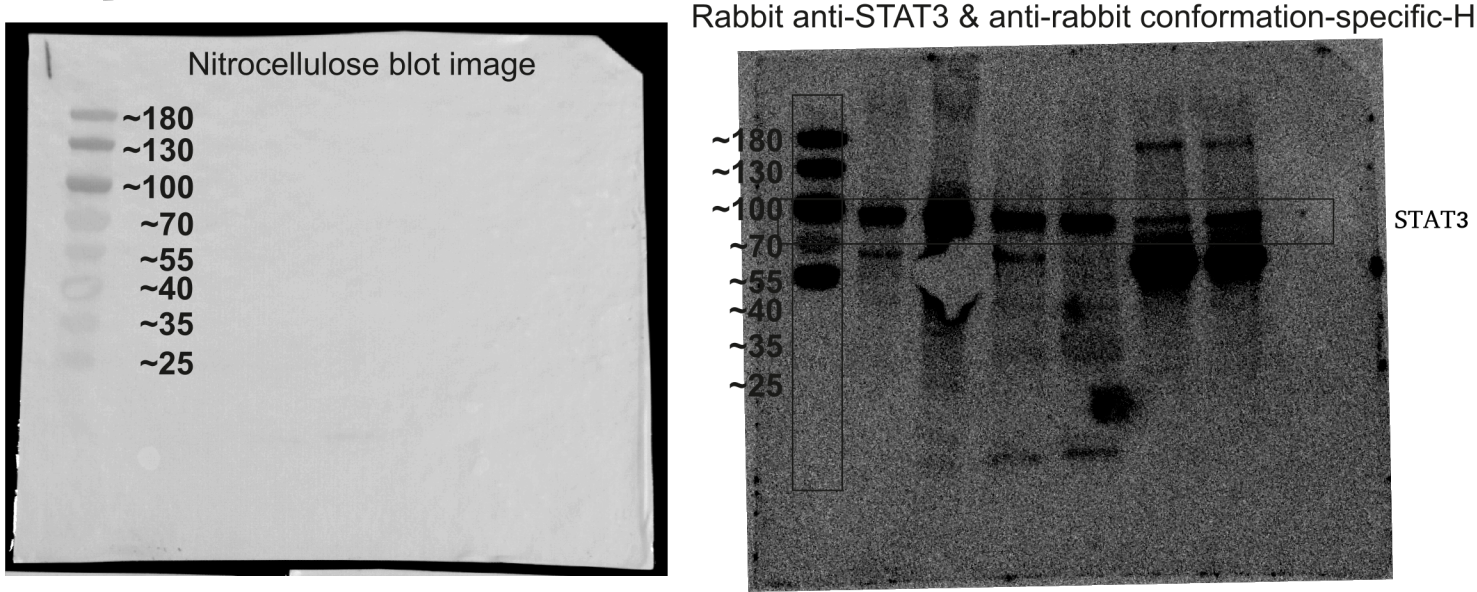
Nitrocellulose blot image
~180
~130
~100
~70
~55
~40
~35
~25
Rabbit anti-STAT3 & anti-rabbit conformation-specific-HRP
~180
~130
~100
~70
~55
~40
~35
~25
STAT3